# 44

Poly EE-83-005

# Optimization of the Design of Electric Traction Motors for Railroad and Other Applications

Enrico Levi
Polytechnic Institute of New York
333 Jay Street
Brooklyn, NY 11201

August 1983

Final Report

Contract No. DTRS5681-C-00023

Prepared for

U.S. Department of Transportation
Research and Special Programs Administration
Washington, DC 20590

**Technical Report Documentation Page**

| 1. Report No. | 2. Government Accession No. | 3. Recipient's Catalog No. |
|---|---|---|
| | | |

| 4. Title and Subtitle | 5. Report Date |
|---|---|
| Optimization of the Design of Electric Traction Motors for Railroad and Other Applications | 6. Performing Organization Code |
| | 8. Performing Organization Report No. |
| 7. Author(s)<br>E. Levi | |
| 9. Performing Organization Name and Address<br>Polytechnic Institute of New York<br>333 Jay Street<br>Brooklyn, NY 11201 | 10. Work Unit No. (TRAIS) |
| | 11. Contract or Grant No.<br>DTRS5681-C-00023 |
| | 13. Type of Report and Period Covered<br>Technical Report (Final)<br>June 1, 1981-August 31, 1983 |
| 12. Sponsoring Agency Name and Address<br>Department of Transportation<br>RSPA<br>Procurement Division, DPA-14<br>400 Seventh Street, S.W., Washington, DC 20590 | 14. Sponsoring Agency Code |

15. Supplementary Notes

16. Abstract

This report summarizes the results of an effort aimed at the optimization of the design of electric traction motors for railroad and other applications. Earlier extensive studies of electric motors for ground transportation were conducted at the Polytechnic over several years. These led to the development of a direct approach to the design. The direct approach is implemented here giving full consideration to the interfaces both with the electrical system, i.e. the power conditioner, and the mechanical system, i.e. the coupling and the gear.

| 17. Key Words | 18. Distribution Statement |
|---|---|
| Traction motors, polyphase, three-phase, induction, synchronous, power conditioner, rectifier, inverter. | |

| 19. Security Classif. (of this report) | 20. Security Classif. (of this page) | 21. No. of Pages | 22. Price |
|---|---|---|---|
| Unclassified | Unclassified | | |

## Executive Summary

At the present time, new electric propulsion systems are being developed for every mode of transportation, with particular reference to railroads. Polyphase (typically three-phase) electric motors are making inroads in a field previously dominated by dc and ac (single-phase) motors. Furthermore, new topologies incorporating permanent magnets and amorphous metals are evolving. In order to optimize the design of these motors, new analytical tools were required and a new direct approach to their design was developed under DOT sponsorship.

The research described in this report expands the scope of this direct approach to include interfacing with the power-conditioning and mechanical transmission. This makes the direct approach applicable to a wide range of electric propulsion systems involving different types of motors.

Contrary to motors supplied at constant frequency and voltage, in traction motors there exists no single point of operation which may serve to define a nominal power and speed. Performance must be optimized over an "envelope" of operating points. Accordingly the design approach was expanded to accommodate indeterminacies in the specifications (e.g. motor speed, frequency, voltage, current) and elasticity in thermal loading (type of insulation, cooling, and duty cycle).

It was found that ac motors fed by inverters behave like dc motors, because the dc source does not "see" the motor reactances. The counterelectromotive force developed by the motor is uniquely defined by the specified load power, efficiency of the mechanical transmission, source voltage, and resistance of the energized circuit. Specific relations were derived for the various types of machines and inverters. Once the emf is determined, the main design problem becomes the selection of its constitutive factors. The trade-offs involved in this selection were determined. Minimization of the volume of the ferromagnetic structure and, therefore, of the weight of the motor leads to an optimal value for the magnetic flux density or "magnetic loading." Instead, the surface current density, or "electric loading," is chosen on the basis of thermal considerations. The relevant relation to the "road-envelope" was established. This led to the formulation of scaling laws which yield the main dimensions of the ferromagnetic structure and of the windings in terms of the performance specifications, within the constraints of the allowable material stresses. These scaling laws permit quick optimization of the overall propulsion system with regard to size, weight, cost, and efficiency.

Drives supplied by solid-state power-conditioners are prone to instability and the torques they develop contain pulsating components. Both features are particularly objectionable in railroads, because they cause wheel slip and degrade locomotive wheel-to-rail adhesion capability. Therefore, the design approach was expanded to include consideration of speed control and harmonics. Microprocessor control

aimed at maintaining the flux constant was deemed to be most likely to ensure stability. An experimental verification effort, outside the scope of the present contract, is in progress. With regard to pulsating torques, the development of gate-turn-off switching elements makes suppression of the harmonics at the source by means of pulse-width-modulation preferable over the alternative of increasing the number of phases.

A major requirement of the power conditioner is reliability, especially during transients. This favors the adoption of synchronous motors, because, when overexcited, they allow for natural commutation. Also favoring the synchronous motor in traction applications is the need for a large air gap between stator and rotor. Weighed against these advantages, in the case of field excitation and brushless constructon, is the need for rotating transformers or a complex topology. As a result of these space requirements, high power synchronous motors cannot be fitted between the wheels in single-axle drives, but must be mounted longitudinally on the truck.

Excitation by means of permanent magnets offers the advantages of high tip speed and efficiency. It is, however, restricted to low power levels by manufacturing difficulties and by magnet space requirements in the rotor. This, together with the destructive short circuit currents which are induced when driven by the wheel under fault conditions, rules out its application in propulsion system for railroads. It may, however, be employed in some electric passenger vehicles and it is ideally suited for auxiliaries and actuators.

This leaves the squirrel-cage induction motor as the best choice for most traction drives. Since frequency and voltage adjustments can provide the desired torque over a wide range of current and speed, the specifications of starting performance and overload capability do not impose particular constraints on the design. It follows that there is no incentive to keep the leakage reactances particularly low, to rely on the use of deep bars for skin-effect enhancement, or to skew the bars in order to prevent crawling and cogging. High leakage inductance and low secondary resistance, however, lead to large time constants and sluggish response. Moreover, even a low secondary resistance at fundamental frequency cannot prevent high losses when harmonic currents are present. This again favors the adoption of pulse-width-modulated inverters.

The design approach thus developed has been applied to two specific drives at the extremes of power level requirements:

(1) The locomotive for a pasenger train operating along the North Eastern corridor

The road envelope leads to the specification of an effective continuous rating of 1500 kW at 3500 rpm. The design shows that the motor can be fitted within the allowable dimensions of 800 cm for both axial length and diameter. The projected performance of the motor compares favorably with that of the BQg4843 motor used in Brown Boveri's DB Class E120 universal mainline locomotive. The power

level which can be developed by one motor is limited mainly by the allowable axial length. This, together with the need for ruggedness, makes it unlikely that higher powers can be achieved with heat pipe cooling.

(2) A passenger electric vehicle

Although such a vehicle should be employed in urban traffic, it is penalized by the requirements of thruway merging and passing duties. As a result the motor must be overdesigned. The load envelope leads to a motor capable of delivering a starting torque of 1139 N-m and a maximum power of 33 kW at 4656 rpm. These performance requirements are met by an oil-cooled two-pole motor weighing about 40 Kg and supplied by a pulse-width-modulated inverter with 180° maximum conduction period. Its size and projected performance are similar to those of a motor built by Eaton for the same purpose.

In conclusion, guidelines for the optimization of the design of electric propulsion systems have been established. These guidelines apply in general to electric drives with particular reference to robots. They are, therefore, likely to benefit a large number of potential users.

TABLE OF CONTENTS

## Work Performed Under Phase II of the Contract

A direct approach to the design of traction motors was developed under contract No. DOT-RC-92022 and is described in the final report for that contract: "Polyphase Traction Motors: A Direct approach to the Design of New Machines," PolyEE81-004, June 1981.

Expansion of this approach to include the power conditioner and the mechanical transmission was developed under Phase I of contract No. DTRS5681-C-00023 and is described in the Phase I (Interim) Report: "Optimization of the Design of Electric Traction Motors for Railroad and Other Applications," PolyEE-82-001, June 1982.

During Phase II of the present contract, general guidelines for the optimization of the design of polyphase traction motors in general, of synchronous motors with permanent magnet excitation, in particular, were formulated. Since these guidelines have more general application, and in order to achieve the widest possible dissemination among potential users, the results of the present investigation are presented in the form of three papers to be presented at technical and scientific meetings and later published in the journals of the Engineering Societies. These are attached as Appendices I, II, and III. Also attached, as examples of the approach described in these papers, are the basic designs for a 1500 kW, 3500 rpm locomotive motor and a 33 kW, 4656 rpm motor for an electric passenger vehicle. These are presented as Appendices IV and V respectively.

Major considerations in optimizing the overall propulsion system are the trade-offs between the design of the motor, the power conditioner, and the mechanical transmission. Even though the power conditioner is the most bulky and costly item, the rapid progress in

developing gate-turn-off devices makes it inadvisable to penalize the motor in order to reduce the complexity of the power conditioner. The same holds true with regard to the mechanical transmission. In electrical passenger vehicles the availability of continuous adjustments in the electric supply frequency makes it unnecessary to use variable transmissions. However, unreasonable demands with regard to thruway merging and passing duties impose the need for a two-speed arrangement. This is better achieved in the gear box, than in the motor.

Harmonics in the voltages and currents supplied by the inverter give rise to pulsating torques which are particularly objectionable in rail-on-wheel applications. Again there seems to be little advantage in alleviating the problem in the motor by increasing the number of phases, rather than suppressing the harmonics at the source by means of pulse-width modulation.

Instability is another problem which should not be addressed by artificially changing the parameters of the motor. Various types of control were subjected to in-depth theoretical investigation within the scope of a doctoral dissertation. Nabae's constant-flux scheme was selected as the most promising. In view of its seriousness the problem of stability was also investigated experimentally outside the scope of the present contract. The existence of unstable regions in parameter space and their boundaries were established in a synchronous motor supplied by a voltage source inverter and in a squirrel-cage motor fed by a current source inverter, when they were operated with an open loop. In both cases considerable improvements in stability were obtained by modifying some of the components of the

inverters. Nevertheless instability could not be eliminated completely, without resorting to microprocessor control. A North Star microcomputer was purchased especially for this project. At the time of this writing a program has been prepared in Fortran language. This program features time sharing between the calculation of the current in the rectifier and firing angle commands for the inverter. In order to save computer time, all calculations are performed with the help of tables stored in the memory bank. However, in order to implement the control scheme the program will have to be translated into assembly language.

Adknowledgments

This report covers work performed at the Polytechnic Institute of New York under Contract No. DTRS5681-C-00023 with the Office of University Research and Special Programs Administration of the U.S. Department of Transportation, Dr. Lloyd J. Money, Director.

The support, comments and direction of the technical monitors, Messrs. Matthew Guarino Jr., M. Clifford Gannett, and Richard Scharr are gratefully acknowledged by the author.

Appendix I

# BASIC DESIGN OF ELECTRICAL MACHINES

Enrico Levi, Senior Member
Polytechnic Institute of New York
Brooklyn, NY 11201

Abstract - Guiding principles of general validity are presented for the design of electrical machines. These lead to the formulation of scaling laws which relate the main dimensions to the most important performance parameters.

## INTRODUCTION

In general the design of electrical machines consists of an initial step of synthesis, followed by a cut-and-try analytical approach to optimization. As a first guess the bore volume is found from the specified torque by making use of proportionality factors which are based on previous experience and differ with the type and size of the machine[1]. These data are of little use if the machine to be designed departs even slightly from the standard ones, a case which is becoming more frequent with the development of new insulating and magnetic materials, topologies, and applications. Moreover, the cut-and-try approach to optimization becomes laborious when, as in the case of adjustable speed drives, the motor must be designed on the basis of a "performance envelope," rather a single point of operation and the optimization process must include the power conditioner, at the electrical port, and the mechanical transmission, at the mechanical one.

In this paper the main dimensions of the machine are obtained from scaling laws which are based on the allowable stresses on the materials. The background is provided by an ideal model[2] in which the actual winding on each side of the gap is replaced by an active conductor of uniform equivalent thickness a. The current in the winding is represented by a surface current K which is sinusoidally distributed along the periphery of the gap. This K interacts with the flux density B to produce, according to Biot Savart's law, a surface force density $f_e$. The electromagnetic force, thus, results from the product of two field quantities: K which is related to the power dissipated in the winding, or copper loss, and is called "electric loading," and B which is related to the losses in the iron and is called "magnetic loading."

## MAGNETIC LOADING

The magnetic flux density B which is relevant to the electromechanical power conversion process and which constitutes the "magnetic loading" is the effective, or rms value of the radial component of B at the air gap. Except for special cases, such as superconducting field excitation and printed windings, this value is determined by the characteristics of the ferromagnetic structure into which the conductors are embedded. A rectilinear segment of such a structure is shown in Fig. 1. As can be seen, the structure consists of a core or yoke of height $h_c$, which serves to provide both physical integrity and a path for the magnetic flux $\Phi_c$, and a slotted portion of height $h_s$ which accomodates the active conductors.

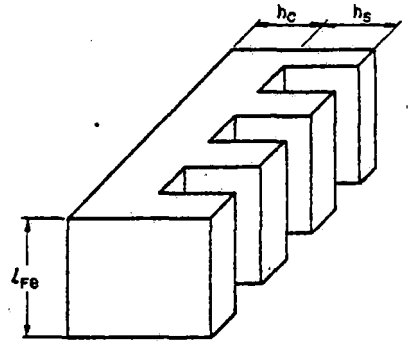


Fig. 1 Segment of magnetic structure.

For a given allowable flux density in the core, $h_c$ is proportional to B or

$$h_c = k^{(c)} B \tag{1}$$

The slot height, instead, represents a compromise between the conflicting requirements of conduction of current in the copper and of flux in the iron teeth. If $w_t$ represents the width of the tooth, $\tau_s$ the slot pitch, and $k_{cu}$ a copper filling factor, given by the ratio of the actual area of the conductors in the slot to the slot area, one can write

$$a\tau_s = k_{cu} h_s(\tau_s - w_t) \tag{2}$$

where a is the effective thickness of the conductor and $k_{cu}$ varies between 0.3 for small machines with round wires and for large high voltage machines, to 0.5 with class F insulation and wires of square cross section.

Since the weight and cost of the machine increases with the volume of the magnetic structure, one is interested in minimizing this volume. This can be achieved[3] by an appropriate choice of the "magnetic loading" B.

Neglecting the curvature of the structure, which is significant only in small machines, and assuming the rectilinear shape of Fig. 1, the electromagnetic force per unit volume of the magnetic structure is

$$\frac{F_e}{(Vol)_{m.s.}} = \frac{\langle f_e \rangle}{h_c + h_s} = \frac{Re[\bar{K}\bar{B}^*]}{h_c + h_s} = \frac{K\, B\cos\alpha}{h_c + h_s} \tag{3}$$

where the surface force density $f_e$ has been assigned an average value consistent with the assumed sinusoidal distribution and $\alpha$ is the angle by which $\bar{B}$ leads $\bar{K}$.

Both $h_c$ and $h_s$ are related to B in the gap by the principle of continuity of flux.

Assuming that all the flux passes through the iron, the flux density $B_t$ in the tooth is related to B in the gap as

$$B_t w_t = B\tau_s \tag{4}$$

Combination of Eqs. (2) and (4) gives

$$h_s = \frac{a}{k_{cu}(1-\frac{w_t}{\tau_s})} = \frac{a}{k_{cu}(1-\frac{B}{B_t})} \quad (5)$$

Introducing Eqs. (1) and (5) into Eq. (3) gives

$$\frac{F_e}{(Vol)_{m.s.}} = \frac{K\,B\cos\alpha}{k^{(c)}B + \frac{a}{k_{cu}(1-\frac{B}{B_t})}} \quad (6)$$

Equating the partial derivative of this relation with respect to B to zero, one finds that the force per unit volume of the magnetic structure attains its maximum values when

$$B = \frac{1}{2} B_t \quad (7)$$

or when $w_t = \tau_s/2$. Since an rms value of $B_t$ in excess of 1.4T would drive the iron too far into saturation, it follows that B is limited to about 0.7T.

In contrast to the magnetic loading, there exists no optimal value for electric loading and the force density increases with increasing K.

## HEAT TRANSFER

In thermal steady state, the energy dissipated into heat in the iron core and in the windings must equal the heat transferred to the cooling medium. The iron loss is easily removed, because of good heat conduction of the laminations. Removal of heat from the windings represents a more difficult problem, because the electrical insulation also represents good thermal insulation, and because the lifetime of the insulation decays exponentially with rising temperature[4,5].

If one denotes by $p_{s\text{-}diss}$ the power dissipated per unit surface of the active conductor and introduces an overall heat transfer coefficient h, the temperature rise of the winding can be written as

$$\vartheta_w = \frac{p_{s\text{-}diss}}{h} \quad (8)$$

The allowable temperature rise depends on the type of insulation and the heat transfer coefficient on the type of cooling. Typical values of h in Watts per degree Kelvin per meter square are

$$h \sim \begin{cases} 200 \text{ to } 250 & \text{for liquid cooling inside the conductor} \\ 70 \text{ to } 130 & \text{for liquid cooling over the conductor} \\ 100 \text{ to } 150 & \text{for heat pipes} \\ 70 \text{ to } 90 & \text{for forced air draft} \\ 30 \text{ to } 50 & \text{for internal air ventilation} \end{cases} \quad (9)$$

The most common cooling medium is air. If $v_a$ denotes the velocity of the air lapping the winding, Luke[6] found empirically that

$$h \sim 20\, v_a^{0.6} \quad [WK^{-1}m^{-2}] \quad (10)$$

In motors with internal air ventilation the air is driven by fans attached to the shaft. It is, therefore, reasonable to expect that the velocity of the air be proportional to the peripheral speed of the rotor, so that the heat transfer coefficient can be written as

$$h = k_h(D\tfrac{rpm}{60})^{0.6} = k_h(D\tfrac{f}{p})^{0.6} \quad (11)$$

where D stands for bore diameter, rpm for revolutions per minute, f for electrical frequency, and p for number of pole pairs. If all dimensions are expressed in SI units, as will be the case in all subsequent equations, a typical value for $k_h$ is 16.

## DESIGN BASED ON THERMAL CONSIDERATIONS

The heat balance Eq. (8) imposes a limit on the output which can be obtained from a machine of a certain size, since the output is related to the copper loss $P_{cu}$ in the winding. If one denotes by $\ell_{co}$ the average length of one conductor and by L the effective length of the lamination stack, Eq. (8) can be rewritten as

$$p_{s\text{-}diss} = \frac{P_{cu}(L/\ell_{co})}{\pi DL} = h\vartheta_w \quad (12)$$

In the design stage this relation serves to determine the bore diameter D as

$$D = \left[\frac{P_{cu}(L/\ell_{co})}{\pi h\vartheta_w (L/D)}\right]^{1/2} \quad (13)$$

where L/D is the aspect ratio of the bore. To find K one can use the torque/power relation

$$T = \pi\frac{D^2}{2} L \langle f_e \rangle = \pi \frac{D^2}{2} LKB\cos\alpha = \frac{p}{2\pi f} P_i \cos\alpha \quad (14)$$

where $P_i$ is an ideal power equal to the rated value divided by $\cos\alpha$ which, if not known, can be approximated by the specified power factor. Introduction of Eq. (13) into Eq. (14) yields

$$K = \frac{p}{f}\frac{P_i}{[P_{cu}]^{3/2}}\left[\frac{h\vartheta_w}{(L/\ell_{co})}\right]^{3/2}\left[\frac{L/D}{\pi}\right]^{1/2}\frac{1}{B} \quad (15)$$

The volume current density J, then, follows from its definition

$$J = \frac{K/k_{dp}}{a} \quad (16)$$

where $k_{dp}$ is a winding factor[1] which takes into account the discrete nature of the active conductor. Accordingly the surface density of dissipated power becomes

$$P_{s\text{-}diss} = \frac{(K/k_{dp})^2}{\gamma a} = \frac{(K/k_{dp})}{\gamma} J = h\vartheta_w \quad (17)$$

Solving for J and making use of Eq. (15), one obtains

$$J = \gamma k_{dp}\frac{f}{p}\frac{[P_{cu}(L/\ell_{co})]^{3/2}}{P_i}\left[\frac{\pi}{h\vartheta_w(L/D)}\right]^{1/2} B \quad (18)$$

The ratio of Eq. (15) for K and Eq. (18) for J, then, yields the equivalent thickness of the active conductor

$$a = \frac{K}{k_{dp}J} = \frac{(L/D)}{\pi\gamma k_{dp}^2}\left[\frac{h\vartheta_w P_i}{Bf/p}\right]^2 \frac{1}{[P_{cu}(L/\ell_{co})]^3} \quad (19)$$

One observes the strong sensitivity of a on the assumptions made with regard to h, $\vartheta_w$ and $P_{cu}$. This is particularly important because a affects the depth of the slot and, hence, the slot leakage.

Guidance for the estimation of the overall heat transfer coefficient was given in the previous section. With regard to $\vartheta_w$, the temperature rise in the windings, at the outset of the design, it is wise to leave some margin of safety. According to ANSI/IEEE Std. 112-1978 "IEEE Standard Test Procedure for Polyphase Induction Motors and Generators," in ascertaining the copper losses, the winding resistances should be calculated at the following temperatures

$$t = \begin{cases} 75°C \text{ for Class A insulation} \\ 95°C \text{ for Class B insulation} \\ 115°C \text{ for Class F insulation} \\ 130°C \text{ for Class H insulation} \end{cases} \quad (20)$$

By subtracting the standard ambient temperature of 40°C one arrives at $\vartheta_w$ values which are about 2/3 of the maximum allowable temperature rise for the selected class of insulation. The design should be based on these values.

The copper loss $P_{cu}$ refers to the conductor which is critically stressed thermally. This usually implies the primary in the induction machine and the armature in the synchronous one. The copper loss can be deduced from the specified efficiency and an assumed partition for the losses. A good starting guess is given by Cigánek[7].

$$P_{cu} = 0.42\ P_i^{0.75} \quad (21)$$

Finally, values must be assigned to L/D and $\ell_{co}/L$. Efficiency considerations would suggest the selection of the aspect ratio L/D which minimizes the winding resistance R for a given electromotive force e i.e. the L/D which minimizes the length of one turn for a given area it encompasses. These considerations lead to

$$\frac{L}{D} \sim \frac{\pi}{2}\ p^{-2/3} \quad (22)$$

Higher values of L/D should be chosen if the specifications call for low rotor inertia or low motor weight.

The ratio of the average length of one conductor to effective bore length is

$$\ell_{co}/L \sim 1 + \frac{2D}{pL} \sim 2.27\ p^{-0.16} \quad (23)$$

Introducing Eqs. (21), (23), (11), and (22) into Eq. (13) gives for an internally ventilated machine

$$D \sim 0.09\ \vartheta_w^{-0.385}\ P_i^{0.29}\ p^{0.55}\ f^{-0.23} \quad (24)$$

Introducing this value of D into Eqs. (22) and (23) one can find L and $\ell_{co}$.

## PERFORMANCE CONSIDERATIONS

It appears that, if B is specified, for instance, by choosing its optimal value according to Eq. (7), then, the surface current K and the main dimensions of the machine can be selected solely on the basis of thermal considerations and a torque equation which essentially expresses Biot Savart's law. However, a selection based on such narrow grounds may not satisfy other performance specifications of the motor.

In both synchronous and induction motors supplied at constant frequency the overload capability is strongly affected by the magnetizing current. Making use of Ampére's law, its per unit value can be found as

$$i_\mu = \frac{2pg}{\mu_o D}\frac{B}{K_R} \quad (25)$$

where g is an effective gap length which accounts for the presence of slots and saturation in the iron[1], $\mu_o$ is the permeability of vacuum, and the subscript R stands for rated value.

In general purpose squirrel-cage motors of NEMA Class A one can assume

$$i_\mu \sim 0.28\ P_i^{-0.1}\ f^{0.15}\ p^{-0.5} \quad (26)$$

In synchronous motors fed at constant voltage and frequency or from naturally commutated inverters is approximately

$$i_\mu \sim 1.27\ C_q \quad (27)$$

where $C_q$ is the reactance coefficient in the quadrature axis[1,4].

Expression of the salient features of the performance in terms of the single parameter $i_\mu$, now allows to combine Eqs. (15) and (25) to uniquely define the effective flux density in the air gap as

$$B = \left(\frac{\mu_o i_\mu}{2f(g/D)}\right)^{1/2} \left(\frac{L/D}{\pi P_i}\right)^{1/4} \left(\frac{h\vartheta_w}{P_{Cu}(L/\ell_{co})/P_i}\right)^{3/4} \quad (28)$$

This equation puts in evidence the dependence of B on the air gap ratio g/D. In induction motors, in which good coupling between primary and secondary is essential, the air gap is made as small as mechanical considerations allow. These lead to

$$\frac{g}{D} \sim 7.25 \times 10^{-3}\ P_i^{0.01}\ p^{-0.5} \quad (29)$$

With the help of this relation one can calculate B, in an induction machine. If B turns out to be smaller than the value given by Eq. (7), then the motor is "thermally limited." In this case B could be raised and, therefore, the motor dimensions reduced, by improving the cooling or by switching to a higher class of insulation.

If, instead, B turns out to be too large, then the motor is "saturation limited." A slight increase in B can be accommodated by increasing the ratio of tooth width to slot pitch $w_t/\tau_s$, according to Eq. (4). This, however, results in longer end windings. Alternatively one must reduce $\vartheta_w$ and pay the price in terms of increased bore dimensions. A lower $\vartheta_w$, however, allows to switch to a less expensive class of insulation and reduces the copper losses, because of better conductivity.

Different considerations hold for a synchronous machine. Here stability requirements and power factor considerations force the selection of an $i_\mu$ which according to Eq. (27) must exceed 2/3. Such an $i_\mu$ is more than twice the value recommended for induction machines by Eq. (25). If the ratio g/D were the same, a synchronous machine with the same magnetic loading B would allow a much smaller electrical loading $K_R$, than an induction machine and, therefore, would be much larger for the same developed torque. It follows that synchronous machines should be built with larger air gaps, than are permitted by purely mechanical considerations, according to Eq. (20). Large air gaps are not as objectionable as in the induction motors, because the availability of a second excitation provided by the field permits maintaining an adequate power factor. Moreover, the field winding can tolerate higher electric loading and thermal stresses, than the armature, because its lower voltage lessens the insulation requirements.

Once the electric and magnetic loadings have been selected, all the dimensions of the bore and of the

winding are determined. Another dimension which is very important, because it determines the frame size is the outside diameter of the laminations

$$D_o = D + 2h_s + 2h_c \tag{30}$$

As a first approximation one may assume

$$D_o \sim (1.1 + \frac{0.8}{p}) D \tag{31}$$

The outside diameter can also lead to a rough estimate of the motor weight and cost. The weight in kg is approximately

$$W \sim 2.63 \times 10^3 D_o^{3.1} \tag{32}$$

and the original equipment manufacturer's cost (OEM) in 1982 $ is approximately 8$/kg.

## CONCLUDING REMARKS

A set of scaling laws based on the thermal and magnetic stresses on the materials allows to relate the main dimensions of the ferromagnetic structure and of the windings to the performance of the machine expressed in terms of its power, frequency, number of pole pairs, and per unit magnetizing current.

These scaling laws are quite general and apply to all modes of operation, motoring, generating, and braking, and to unconventional, as well as conventional machines.

Although the basic design must be checked by verifying all the parameter values on which it was based, it provides all the information which is needed for the optimization of the overall drive.

## ACKNOWLEDGMENT

Part of the work reported in this paper was supported by the U.S. Department of Transportation under Contract No. DTRS5681-C-00023.

## REFERENCES

[1] M. Liwschitz-Garik, and C.C. Whipple, A-C Machines, Van Nostrand, Princeton, 1961. Reprints available from Robert E. Krieger Publishing Co. Inc., Box 9542, Melbourne, FL 32901.

[2] E. Levi, and M. Panzer, Electromechanical Power Conversion, 2nd English Edition Dover Publications Inc., New York 1974. Reprints available from Robert E. Krieger Publishing Co. Inc. (See above Ref.)

[3] H. Weh, "High Power Synchronous Machines with Permanent Magnet Excitation," Proc. International Conference on Electrical Machines, Sept. 15-17, 1980, Athens, Greece, pp. 295-303.

[4] M. Kostenko, and L. Piotrovsky, Electrical Machines, Foreign Languages Publishing House, Moscow.

[5] J.H. Walker, Large Synchronous Machines, Clarendon Press, Oxford, 1981.

[6] G.E. Luke, "Surface Cooling of Electrical Machines in Strong Air Current," AIEE Trans. p. 1036, 1926.

[7] L. Cigánek, Stavba Electrických Stroju SNTL, Praha, 1958.

Appendix II

# DESIGN CONSIDERATIONS FOR MOTORS USED IN ADJUSTABLE-SPEED DRIVES

Enrico Levi
Polytechnic Institute of New York
Brooklyn, NY 11201

Abstract:

In adjustable-speed drives the constraints imposed on the motor at its electrical and mechanical port are not fixed, but subject to change. It is found that the counterelectromotive force developed by the motor is uniquely defined by the specified load power, efficiency of the mechanical transmission, source voltage and resistance of the energized circuit.

In this respect ac motors fed by inverters behave like dc motors, because the dc source does not "see" the motor reactances. Relations are derived for the various machines and inverter types. With the emf determined, the main design problem becomes the selection of its constitutive factors.

The involved trade-offs are examined for the extreme cases of drives requiring maximum torque at top speed and at stalling.

## 1. Introduction

An adjustable-speed drive in general consists of a power conditioner, a motor, and a mechanical transmission or gear. Contrary to motors supplied at constant frequency and voltage, in adjustable-speed drives there exists no single point of operation which may serve to define a nominal power and speed. Performance must be optimized over a duty-cycle, or an envelope of operating points.

These envelopes are usually described in terms of torque-speed characteristics of which extreme cases are:

(a) Torque increasing with increasing speed, as in drives for centrifugal pumps, blowers, and compressors

(b) Torque decreasing with increasing speed, as in high inertia drives requiring high accelerating torques. A typical application is electric traction.

The drive must satisfy the prescribed torque-speed characteristics over the time duty-cycle without exceeding the allowable temperature rises. The temperature rise depends on the type of ventilation and, in this respect too, adjustable-speed drives differ from fixed-speed ones, because usually they need separate blowers. This provides the designer with more latitude, but makes the task of optimization more difficult, because of the larger number of variables which are involved.

## 2. Load Power and Emf

The general case of a motor connected to a load through a gear is considered. At all times the power required at the load shaft, and denoted by $P_L$, must be balanced by the power developed by the motor. Expressing the torque in terms of Kron's generalized machine theory[1], one can write:

$$P_L = \Omega_L T_L = \frac{2\pi n_L}{60} r\eta_t \, [i]_t^* \, [G] \, [i] \qquad (1)$$

where $\Omega_L$ = angular velocity at the load shaft

$T_L$ = torque at the load shaft

$n_L$ = load speed in rpm

$r$ = gear ratio

$\eta_t$ = efficiency of the mechanical transmission or gear

[i] = matrix of the winding currents

$[i]_t^*$ = current matrix transposed and conjugate

[G] = torque matrix

The components of the current matrix [i], in general, vary with time on a fast scale with frequency

$$f = \frac{rn_L p}{60(1-S)} \tag{2}$$

where p = number of pole pairs in the motor

$$S = \text{slip} = \frac{n_{Ls}-n_L}{n_{Ls}} \tag{3}$$

and the subscript s stands for synchronous. In synchronous motors $n_{Ls} = n_L$, hence, S = 0.

The currents are related to their sources as

$$\bar{i} = \frac{\bar{V}_s-\bar{e}}{\bar{Z}_s+\bar{Z}} \tag{4}$$

where $\bar{V}_s$ = Thevenin equivalent source voltage

$\bar{Z}_s$ = Thevenin equivalent source impedance

$\bar{Z}$ = impedance of the winding through which i flows

$\bar{e}$ = electromotive force

If one observes that, in general, all variables in Eq. (4) vary slowly in amplitude with time, it follows that the amplitude of the currents also vary with time on a slow scale.

The torque matrix [G] contains the inductances of the windings, which are functions of their characteristics and of the dimensions of the motor.

The electromotive force e is related to the magnetic flux by Faraday's law as[2]

$$e = 2\pi f N_{eff} \Phi = \frac{2\pi}{60} n_L r N_{eff} p \Phi \qquad (5)$$

where $N_{eff}$ = effective number of series connected turns

$\Phi$ = flux per pole

When Eqs. (4) and (5) are inserted into Eq. (1) and [G] [i] is expressed in terms of the flux per pole $\Phi$, then all the quantities defining e in Eq. (5) appear as a group. This is easily verified in the case of a dc machine, because impedances reduce to resistances and complex quantities reduce to real numbers.

In a dc machine the torque is[2]

$$T = \frac{2}{\pi} N I_a p \Phi \qquad (6)$$

where N is the number of series connected turns per parallel branch and $I_a$ is the armature current. The electromotive force is[2]

$$e = \frac{4}{60} n_L r N p \Phi \qquad (7)$$

so that Eq. (1) becomes

$$P_L = \frac{2\pi n_L}{60} r\eta_t \left(\frac{2}{\pi} N I_a p \Phi\right) = \eta_t e \frac{V_s - e}{R_s + R_a} \qquad (8)$$

Solving for e and introducing a conversion efficiency $\eta_c$ yields

$$e = \eta_c V_s = \frac{1}{2}\left[1 + \sqrt{1 - \frac{4(R_s+R_a)P_L}{\eta_t V_s^2}}\right] V_s \qquad (9)$$

Recognition that the conversion efficiency must be high leads finally to

$$e \sim \left[1 - \frac{(R_s+R_a)P_L}{\eta_t V_s^2}\right] V_s \qquad (10)$$

This equation determines the value of the emf and the resistances of the armature circuit, for specified source voltage, load power and transmission efficiency.

3. Inverter-fed Motors

Very similar relations are obtained with inverter-fed ac motors, because the dc source "sees" only the elements of the load which consume real power. As a result the motors can be represented by resistive equivalent circuits similar to that of a dc machine[3,4]. With this in mind Eq. (10) can be rewritten as

$$e_{dc} \sim \left[1 - \frac{(R_s+R_a)P_L}{\eta_t V_s^2}\right] V_s \qquad (11)$$

where the subscript dc denotes ac quantities referred to the dc side. The reduction factors to the dc side are obtained by applying the principle of conservation of energy.

Three cases will be considered:

(1) current-source inverter with $2\pi/3$ conduction period

(2) voltage-source inverter with $2\pi/3$ conduction period

(3) voltage-source inverter with $\pi$ conduction period

The ratio of the rms value of the fundamental to the amplitude of the rectangular wave is $\sqrt{6}/\pi$ in cases (1) and (2) and $\frac{\sqrt{2}}{\pi}$ in case (3). Therefore, with 3-phase, star connected windings one obtains for each case, as denoted by the appropriate subscript

$$\left(\frac{I_{ph}}{I_{dc}}\right)^{(1)} = \frac{\sqrt{6}}{\pi}$$

$$\left(\frac{V_{ph}}{V_{dc}}\right)^{(2)} = \frac{1}{2}\ \frac{\sqrt{6}}{\pi} \tag{12}$$

$$\left(\frac{V_{ph}}{V_{dc}}\right)^{(3)} = \frac{\sqrt{2}}{\pi}$$

Equating the ac and dc powers, then, yields

$$\left(\frac{V_{ph}}{V_{dc}}\right)^{(1)} = \frac{1}{3\sqrt{6}}\ \frac{\pi}{\cos\phi}$$

$$\left(\frac{I_{ph}}{I_{dc}}\right)^{(2)} = \frac{1}{3}\ \frac{2}{\sqrt{3}}\ \frac{\pi}{\cos\phi} \tag{13}$$

$$\left(\frac{I_{ph}}{I_{dc}}\right)^{(3)} = \frac{1}{3\sqrt{2}}\ \frac{\pi}{\cos\phi}$$

and

$$\left(\frac{R_{dc}}{R_{ph}}\right)^{(1)} = 3\left(\frac{\sqrt{6}}{\pi}\right)^2 = \frac{18}{\pi^2}$$

$$\left(\frac{R_{dc}}{R_{ph}}\right)^{(2)} = \frac{1}{3}\left(\frac{2\pi}{\sqrt{3}\cos\phi}\right)^2 = \frac{2\pi^2}{9\cos\phi^2} \tag{14}$$

$$\left(\frac{R_{dc}}{R_{ph}}\right)^{(3)} = \frac{1}{3}\left(\frac{\pi}{\sqrt{2}\cos\phi}\right)^2 = \frac{\pi^2}{6\cos\phi^2}$$

In assigning a value to $V_{dc}$ one must subtract the forward voltage drop $V_f$ across the switching elements.

In the case of a squirrel-cage motor, if the magnetizing current is neglected, the active part of the equivalent circuit reduces to

$$R_1 + R_2' + \frac{1-S}{S} R_2' \tag{15}$$

where $R_1$ = primary resistance

$R_2'$ = secondary resistance referred to the primary

and S is the slip of the rotor past the revolving field. Therefore the electromotive force referred to the dc side becomes

$$e_{dc} \sim \frac{1-S}{S} (R_2')_{dc} I_{dc} \tag{16}$$

In the case of a synchronous motor fed by a current-source inverter it is expedient to express the power in terms of the field excitation current referred to the armature $I_f'$, the armature current $I_a$, and the angle $\beta$ by which $\bar{I}_f'$ leads $\bar{I}_a$. The power balance is then

$$V_{dc} I_{dc} \sim 3R_a I_a^2 - 3(\omega M_f I_f' I_a \sin\beta + \frac{\omega(M_d - M_q)}{2} I_a^2 \sin 2\beta) \tag{17}$$

where $\omega$ = $2\pi f$ = radian frequency

$R_a$ = armature resistance per phase

$M_f$ = field inductance

$M_d$ = direct axis inductance

$M_q$ = quadrature axis inductance

Introducing the first of Eqs. (12) and dividing by $I_{dc}$, one obtains:

$$V_{dc}^{(1)} \sim \frac{18}{\pi} R_a I_{dc} - \frac{18}{\pi} \left[ \frac{\omega(M_d - M_q)}{2} \sin 2\beta \right] I_{dc}^{(1)} - \frac{3\sqrt{6}}{\pi} \omega M_f I_f' \sin\beta \tag{18}$$

where the last term can be identified as a voltage source and the second term in the square brackets may be considered as an equivalent resistance which accounts for the power contributed by the variable reluctance effect. The electromotive force referred to the dc side $e_{dc}$ is the voltage behind the transformed armature resistance.

Finally, when the synchronous motor is fed by a voltage-source inverter, the power should be expressed in terms of the field emf $e_f'$, the armature voltage $V_a$, and the power angle $\delta$ by which $\bar{e}_f'$ leads $\bar{V}_a$. Neglecting the armature resistance, the power balance gives[2]

$$I_{dc}^{(2)} = -3\sqrt{\frac{3}{2}}\ \frac{1}{\pi}\frac{1}{\omega(L_a M_d)} e_f' \sin\delta - \frac{9}{2\pi}\frac{M_d - M_q}{\omega(L_a+M_d)(L_a+M_q)}\frac{\sin 2\delta}{2} V_{dc}^{(2)} \tag{19}$$

and

$$I_{dc}^{(3)} = -3\sqrt{\frac{2}{\pi}}\ \frac{1}{\omega(L_a M_d)} e_f' \sin\delta - \frac{6}{\pi}\frac{M_d - M_q}{\omega(L_a+M_d)(L_a+M_q)}\frac{\sin 2\delta}{2} V_{dc}^{(3)} \tag{20}$$

where the first term on the right hand side can be identified as a current source and the second as representing a shunting conductance. It follows that $V_{dc}$ can be identified with $e_{dc}$. It is interesting to note that the sign of the equivalent resistance due to saliency effects depends on whether or not $M_d$ is larger than $M_q$ and, therefore, is opposite in machines with permanent magnet and current excitation[3].

## 4. Functional Dependence of the Emf

The performance of adjustable-speed drives is usually specified in terms of maximum performance envelopes. These specify the load torque $T_L$ and speed $n_L$ as functions of time over given duty cycles.

In contrast, the variation of $V_s$, $\Phi$ and R with time are subject to optimization. According to Eqs. (4) and (5), changes in $V_s$ and $\Phi$ are needed to control the speed. In the case of the dc motor, R changes abruptly when the chopper is by-passed at the end of the starting phase. With ac motors, instead, the power conditioner must remain connected at all times. The resistances, however, are replaced by impedances which become functions of time, through their dependence on frequency, and in the case of traction motors for electric railroads, because of the changing distance from the substation.

Equations (12) through (20) establish a one-to-one correspondence between the parameters of various types of inverter drives and a dc motor drive. In particular, they establish an equivalent electromotive force $e_{dc}$ which can be transformed into $e_{ph}$ by using the appropriate voltage conversion factor from Eqs. (12) and (13). Once $e_{ph}$ has been determined, the main design problem is how to split it into the components which appear in Eq. (5).

First, one must realize that e depends on a combination of quantities having different degrees of variability. At one extreme is the load speed which is the only true independent variable. At the other extreme are the bore diameter D and effective length L which relate the flux $\Phi$ to the effective (rms) value of the magnetic flux density B as

$$\Phi = \frac{DL}{p} B \tag{21}$$

The bore dimensions are fixed at the design stage. B is subject to strict limitations, because of iron saturation. It is, therefore, an index of the magnetic stress or "magnetic loading" of the machine.

Moreover, as can be seen by introducing Eq. (21) into Eq. (5), the number of pole pairs p drops out of the picture as a determining factor of the emf e.

Theoretically the gear ratio r and the effective number of turns $N_{eff}$ are subject to change. However, the cost of the power conditioner hardly justifies additional expense for a variable mechanical transmission or a special switch gear for changing the winding connections, for instance from star to delta, or series to parallel.

## 5. Maximum Performance Envelopes

It follows from the previous considerations that e varies with $n_L$ and B only. The mode of its variation depends on the drive. In drives of type (a), as the speed increases, so do the torque and, therefore, the power. The maximum performance requirements for which motors are designed, thus, occur at maximum speed or, as it is called, at Test Block (TB) point. Most often, however, these drives are operated with Maximum Continuous Rating (MCR) at a speed which may be lower by as much as 30 percent, and, consequently, with much lower power requirements. To obtain the specified torque at TB point, the motor iron is driven far into saturation, so that at TB point the motor is "saturation limited." At MCR point, instead, B is reduced, in order to reduce the magnetizing current requirements. Thus, at maximum continuous rating, the iron losses which are roughly proportional to the product of f and B are small and the copper losses become the predominant ones. Since these losses are the factor determining the temperature rise of the winding, at MCR, the design of the motor is guided by thermal considerations and the

motor is said to be "thermally limited." Operationally, these changes in stress are achieved by controlling the frequency and current, or according to Eqs. (4) and (5), by controlling the coordination between source voltage and frequency.

Coordination between source voltage and frequency is also used in the operation of the high inertia drives of class (b), but with different aims. Here maximum torque is required at starting and, therefore, in the low-speed range. Even though during the starting phase the motor is driven far into saturation, in order to obtain the required high torque, the iron losses are not very significant, because of the low frequency. The current is maintained constant at the highest possible level and this according to Eq. (4) means that the source voltage $V_s$ must be raised in proportion to the speed. The starting phase ends when the voltage reaches its rated value at a speed called base speed. Above this speed, in the running speed range, voltage, current and, therefore, power are maintained constant. According to Eq. (4) this means that e is also kept constant so that, as Eq. (5) shows, the subsequent increase in speed comes at the expense of the flux $\Phi$. It should be noted by comparing Eqs. (16) and (18) that, contrary to the synchronous machine, the emf e of the squirrel-cage motor does not exhibit an explicit dependence on the frequency and, therefore, the speed. As Eq. (5) shows, this implies that, with constant voltage, squirrel-cage motors tend to operate naturally in the field weakening mode.

This kind of operation is depicted in Figure 1. Since the current is maintained practically constant, so are the copper losses and the motor is thermally limited throughout the whole speed range.

## 6. Design Trade-offs

At the design stage, selection of the base speed represents the most critical choice. From the operational point of view a base speed as low as possible is desirable, because it yields the highest starting torque for the rated current and because it allots the largest speed range to speed control by means of field weakening. This, in general, results in energy savings, because it extends the zone which can be utilized for regenerative braking by forcing the field. Moreover, in dc and synchronous machines, field control handles less power and, therefore, it is cheaper. In particular with dc machines, a low base speed extends the speed range in which the chopper can be by-passed.

The trade-offs involved in the choice of a low base speed become apparent from an examination of Eq. (5). For the maximum available source voltage $V_s$ and, therefore, emf e and for a given gear ratio r, the total flux $2p\Phi$ and the effective number of turns $N_{eff}$ increase in inverse proportion to the base speed. The total flux can be made larger only by increasing the bore surface, since B at base speed is still maintained at its highest value allowed by iron saturation. As for increasing $N_{eff}$, it should be noted that the winding impedance Z increases as the square of $N_{eff}$. According to Eq. (8), this reduces the power delivered to the load. Also the space wasted for turn insulation increases in proportion to $N_{eff}$.

In the final analysis the number of series connected turns N serves to match the impedance of the winding to the impedance level of the source and plays a role similar to the turns ratio in a transformer.

The gear ratio r plays a similar role. Since the product $p\Phi$ is proportional to the bore area and, hence, to the dimensions of the motor, it is clear that it is desirable to make r as high as possible in order to achieve the smallest motor size. The limiting factor is, then, the permissible speed of the motor at the highest load speed $n_{Lmax}$. If $n_{max}$ indicates the maximum allowable speed, the gear ratio is

$$r = \frac{n_{max}}{n_{Lmax}} \tag{22}$$

A fixed gear ratio imposes severe demands on the starting performance of the motor, because the maximum starting torque is uniquely determined as

$$T_{st} = \frac{(T_L)_{st}}{r} \tag{23}$$

In many instances $T_{st}$, and not the peak power, becomes the determining factor for the dimensions of the motor. In this case one must weigh the cost effectiveness of a two-speed gear box.

In general r is chosen on the basis of trade-offs which involve consideration of noise level, durability, maintenance, weight and cost, and partitioning of the losses among the gear, power conditioner, and motor, and between the copper and iron in the motor.

## 7. Selection of the Number of Poles

Although the number of pole pairs p does not show up explicitly when the emf is expressed in terms of the magnetic loading B, it is, nevertheless, an important design parameter. First of all, according

to Eq. (2), p is a factor tying the mechanical speed $n_L$ to the electrical frequency f. It has, moreover, other implications.

Up to this point, only one of the integral variables, the emf, has been related to a field quantity, the magnetic loading B. However, the current i also has its field counterpart at the bore surface. This is the surface current density K, which is an index of the copper losses and therefore of the temperature rise in the winding. It is called "electric loading" and is related to i as[5]

$$K = \frac{2mN_{eff}}{\pi D} \; i \qquad (24)$$

where m = number of phases in the winding

According to Biot-Savart's law the product KB gives the force per unit surface of the bore $f_e$. Assuming that both K and B are sinusoidally distributed along the periphery of the gap, the average value of the force density can be expressed as

$$\langle f_e \rangle = \text{Re}\,[\bar{K}\bar{B}^*] = KB \cos\,(\bar{K}\hat{\ }\bar{B})]$$

As a result the total torque can be expressed in terms of the electric and magnetic loadings as

$$T = \frac{D}{2}\,(\pi DL)\,KB \cos\,(\bar{K}\hat{\ }\bar{B})$$

The flux and current densities are not independent. They are related through Ampére's law to one another and to the width of the air gap which separates stator from rotor. Introducing for the gap an effective width g that accounts for the presence of the slots and saturation of the iron, one can write:

$$B = \frac{\mu_o D}{2pg} K_\mu \tag{25}$$

where $\mu_o$ is the permeability of vacuum and the subscript $\mu$ stands for magnetizing. The magnetizing current density $K_\mu$ can be replaced by its rated value $K_R$, by observing that K is proportional to i. The result is

$$\frac{B}{K_R} = \frac{\mu_o D}{2pg} \frac{i_\mu}{i_R} = \frac{\mu_o D}{2pg} i_{\mu p.u.} \tag{26}$$

where $i_{\mu p.u.}$, the per unit value of $i_\mu$, is a performance characteristic of the motor. This equation shows that, with given B, $i_\mu$, and bore dimensions, $K_R$ increases in proportion to p. This puts in evidence a trade-off between magnetic and electric loadings. Machines with a small number of poles, such as induction motors will tend to exhibit large magnetic loadings and machines with a large number of poles, such as synchronous machines, will tend to exhibit large electric loadings.

In conclusion, with low p, the frequency is low but B is high, so that on balance the core losses are not affected by p. In general, consideration of the power factor and commutating reactance tend to favor a small number of poles. However, the choice of p = 1 should be avoided whenever possible, because of manufacturing difficulties and poor performance. Cost, end-turn bracing, fault-currents, and pulsating torque considerations tend to favor a large number of poles.

## 8. Concluding Remarks

A method has been outlined for determining the main dimensions of a motor and of its windings. The method is based on a number of assumptions and approximations which must be verified in a second stage of the design. However, the need to accommodate an integer number of turns per coil will foil any attempt to improve the accuracy of the results by increasing the accuracy of the input data.

Use of Eq. (5) as a basis for the determination of the bore dimensions in terms of its surface

$$\pi DL = 30 \frac{e}{n_L r N_{eff} B} \tag{27}$$

is advantageous, because it forces early selection of $N_{eff}$ and, therefore, of the number of turns per coil. For instance, in the design of a 32 kW motor for an electric vehicle, the choice boils down to one or two turns per coil yielding bore surfaces which differ by a factor of two.

The limitation on the number of values that can be assigned to $N_{eff}$ has an even more critical bearing on the electric loading K. Introduction of Eq. (27) into Eq. (24) yields

$$K = \frac{m N_{eff}^2 n_L r B}{15 e / I} L \tag{28}$$

This shows that K is proportional to the square of $N_{eff}$. Also of interest, because of its bearing on the selection of the aspect ratio D/L, is the proportionality between K and L.

References

1. G. Kron, Tensors for Circuits, Dover Publications, Inc., New York, 1959.

2. S.A. Nasar and L.E. Unnewehr, Electromechanics, and Electric Machines, John Wiley, New York, 1983.

3. D.W. Novotny, and T.L. King, "Equivalent Circuit Representation of Current Inverter Driven Synchronous Machines," Trans. IEEE Vol. Pas-100, pp. 2920-2926, 1981.

4. M. Abbas and D.W. Novotny, "Stator Referred Equivalent Circuits for Inverter Driven Electric Machines," Conference Record, IEEE/IAS Annual Meeting, October, 1978.

5. E. Levi and M. Panzer, Electromechanical Power Conversion, 2nd English Edition, Dover Publications, Inc., New York, 1974. Reprint available from Robert E. Krieger Publishing Co., Inc., Box 9542, Melbourne, FL 32908.

Acknowledgment

This work was supported in part by the U.S. Department of Transportation under Contract No. DTRS5681-C-00023.

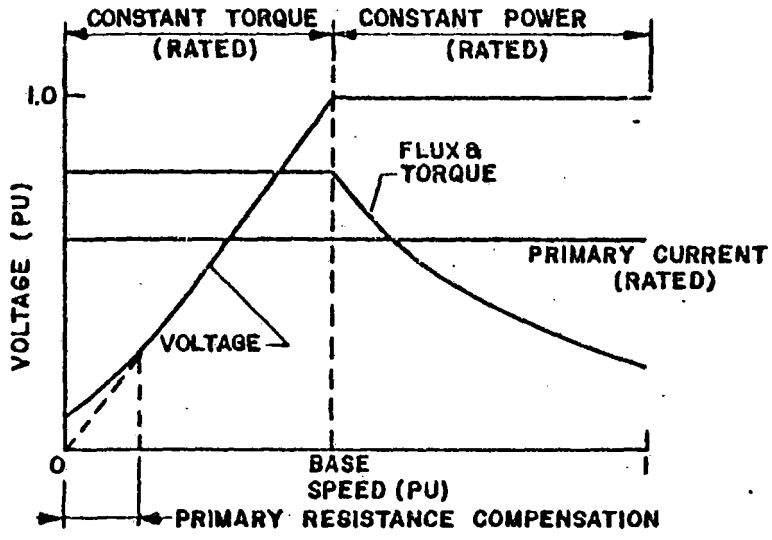


Fig. 1. Voltage, current, and torque as a function of speed in a high-inertia drive.

## List of Captions

Fig. 1. Voltage, current, and torque as a function of speed in a high-inertia drive.

# DESIGN OF POLYPHASE MOTORS WITH PM EXCITATION

Alexander Levran
Teledyne Inet
Torrance, CA 90509

Enrico Levi
Polytechnic Institute of New York
Brooklyn, NY 11201

## Abstract

This paper presents design guidelines for synchronous motors with permanent magnet excitation. A general model is established and the dependence of the electric and magnetic loadings on the angle between the armature and field excitations is put in evidence. For this angle there exists an optimal value which yields maximum torque for maximum allowable flux density in the teeth. Another value yields the minimum volume for the permanent magnets. These values guide the selection of the operating point of the motor and its preliminary design. It is found that, when the pole pitch exceeds a certain value, the magnet requires more space than a current carrying winding.

## 1. Introduction

Field excitation of synchronous motors by means of permanent magnets (PM) offers several advantages over the conventional current excitation. Foremost, it allows rotor speeds which are as high as those of squirrel-cage motors. Moreover, it eliminates the copper losses in the field. This is particularly important at low power levels at which the efficiency is relatively low. Also, as will be shown, in smaller machines permanent magnets occupy less space than field windings and, therefore, lead to more compact designs. It is, thus, to be expected that the market penetration of PM excited motors will

increase, especially in application to robots, where the accurate positioning, which synchronous operation can provide, is important.

The permanent magnets are usually located in the rotor, so that the machine can be made brushless. As shown in Fig. 1, in the rotor the magnets must compete for space with the shaft, the damper winding which is generally in the form of a full squirrel-cage, and the flux barriers which are designed to limit the leakage flux through magnetic short-circuits around the edges of the magnets. In addition the rotor must have sufficient mechanical strength to resist centrifugal forces. Another problem arises from the fact that, especially with ferrites, the flux density that is attainable in the magnet is lower than the one that is desirable in the air gap. It follows that the flux must be concentrated by letting the magnets have a larger cross section than the poles.

These problems have engendered a variety of arrangements for the magnets. They may be placed adjacent to the end faces of the lamination stack, with axes parallel to the axis of rotation, or in its interior. In the latter case, they may be oriented with their axes aligned with the direct axes, so that each magnet provides the whole flux of one pole as shown in Fig. 1, or with their axes oriented in the azimuthal direction as sketched in Fig. 2. In the latter case the magnets extend in the radial direction and fill the interpolar space. This location, which is similar to that of the field windings in a current excited machine, allows the flux of one pole to be contributed by two magnets, instead of one. To further increase the ratio of magnet width to pole pitch, the magnets are often offset from the radial direction, so that they can be extended over the shaft. A

disadvantage of these flux concentration arrangements is that the shaft must be made of nonmagnetic material. For this reason, it is sometimes preferred to increase the cross section of the magnets, by increasing their axial length, rather than their width. In this case the rotor is made to project beyond the stator lamination stack.

In general the magnets have rectangular cross section, but other shapes, such as circular arc and tear drop, have also been used.

The presence of low permeability materials in the d-axes of PM machines causes their direct axis reactance $X_d$ to be low. Therefore, they can be built with air gaps as short as mechanical considerations allow. They also need not be operated with leading current, because of their relatively low power levels; their contribution to power factor compensation would be insignificant and, if they were fed by inverters, these could employ gate turn-off switches, instead of naturally commutated thyristors. While the resulting low excitation requirements are an advantage, the rigidity of PM excitation and the strong coupling between field and armature stemming from the very narrow air gap present the designer with challenging problems. These come in addition to a serious problem arising from limited space availability, i.e. iron saturation and its sensitive dependence on the point of operation.

## 2. Basic Model

The configuration of the magnetic circuit in the direct axis of a PM machine is sketched in Fig. 3 where the following notation has been used:

| | | | |
|---|---|---|---|
| | F | = | mmf |
| | $\Phi$ | = | flux |
| | R | = | reluctance |
| subscript | g | = | gap |
| " | $\ell$ | = | leakage |
| " | M | = | magnet |
| " | a | = | armature |
| " | d | = | direct axis. |

This configuration leads[1,2] to the Thevenin equivalent circuit of Fig. 4. Here the source voltage should be interpreted as

$$V_o = X_{ad} F'_M = C_d X_m F'_M \tag{1}$$

where $X_{ad}$ and $X_m$ are the direct axis and magnetizing reactances of a current excited machine having the same dimensions. $F'_M$, the magnet mmf referred to the armature, is

$$F'_M = \frac{a}{a+b+ab} k_f F_M \tag{2}$$

where $a = \frac{R_\ell}{R_g}$ = ratio of leakage to gap reluctance

$b = \frac{R_M}{R_g}$ = ratio of magnet to gap reluctance

and $k_f$ is the conversion factor of field mmf to the armature in a current excited machine. It is given by

$$k_f = \frac{C_f}{\sqrt{2}\ C_d} \frac{\pi p}{m N_{eff}} \tag{3}$$

where $C_f = \frac{X_{af}}{X_m}$

$p$ = number of pole pairs

$m$ = number of phases

$N_{eff}$ = effective number of turns per phase

and $X_{af}$ is the mutual reactance between armature and field in a current excited machine of the same dimensions.

The series reactance should be interpreted as

$$X_d = \frac{a+b}{a+b+ab} X_{ad} + X_a \tag{4}$$

where $X_a$ is the leakage reactance of the armature.

It should be noted that $V_o$ and $X_d$ reduce to those of a current excited machine in the limit $R_M \to 0$, or $b \to 0$.

The equivalent circuit of Fig. 4 and a similar but sourceless one for the quadrature axis lead to the phasor diagram of Fig. 5(a), where the armature resistance and core losses have been neglected. This diagram is the same as for a current excited synchronous machine except that account has been taken of the fact that $X_d < X_q$.

For design purposes it is expedient to replace the terminal variable voltages and currents by their field counterparts, the magnetic flux density B and the current density K at the bore surface, as shown in Fig. 5(b). B is an index of the saturation in the iron and of the core losses. It is therefore called "magnetic loading." K, instead is an index of the copper losses and, therefore, of the temperature rise in the winding. It is called "electric loading."

The scaling parameters in the transition from terminal to field variables are functions of the bore diameter D and effective length L, in addition to the details of the windings. They are:

$$\frac{e}{B} = 2\pi f \frac{N_{eff}}{\pi p} (\pi DL) \tag{5}$$

where f = electrical frequency

for the emf's e and

$$\frac{I}{K} = \frac{\pi D}{2mN_{eff}} \tag{6}$$

for the current I

Equation (5) is an expression of Faraday's law and Eq. (6) follows from the definition of the surface current density. A flux density B is related to its exciting current density K by Ampére's law, as

$$B = \frac{\mu_o D}{2pg} K \tag{7}$$

where $\mu_o$ = permeability of vacuum

and g is an effective air gap length which takes into account the presence of the slots and the mmf drop along the iron portion of the magnetic flux path.

According to Biot-Savart's law, the electric and magnetic loadings K and B are the components of the force per unit area of the bore surface

$$f_e = KB \tag{8}$$

so that, taking into account the sinusoidal distribution of these quantities along the periphery of the bore, one can write for the total torque

$$T = \frac{P}{2}(\pi DL)\langle f_e \rangle = \frac{P}{2}(\pi DL)\,\mathrm{Re}\{\bar{K}\bar{B}^*\} = \frac{\pi}{2} D^2 L\, KB \cos\alpha \qquad (9)$$

Applying the law of sines to the triangle of flux densities B in Fig. 5(b), one obtains the following relations between B, $B_f$, $B_a$, and $K_a$

$$\frac{B}{\cos\psi} = \frac{C_q B_a}{\sin|\psi-\alpha|} = \frac{B_f + (C_q - C_d')B_a \sin|\psi|}{\cos\alpha} \qquad (10)$$

where $C_d' = \frac{a+b}{a+b+ab} C_d$

$B$ = rms value of the flux density in the air gap at the armature surface

$B_f$ = rms value of field excitation wave

$B_a$ = rms value of the armature excitation wave

$\psi$ = angle by which $\vec{B}_f$ leads $\vec{K}_a$

$\alpha$ = angle by which $\vec{B}$ leads $\vec{K}_a$

Making use of the first relation one obtains for the electric loading

$$K_a = \sqrt{\frac{2p(g/D)}{\mu_o}} \sqrt{\frac{\sin|\psi-\alpha|}{C_q \cos\alpha}} \sqrt{\frac{\langle f_e \rangle}{\cos\alpha}} \qquad (11)$$

and for the magnetic loading

$$B = \sqrt{\frac{\mu_o}{2p(g/D)}} \sqrt{\frac{C_q \cos\psi}{\sin|\psi-\alpha|}} \sqrt{\frac{\langle fe \rangle}{\cos\alpha}} \qquad (12)$$

It appears that, for given dimensions and specified torque and $\alpha$, both $K_a$ and B are strong functions of $\psi$. As $\psi$ increases, $K_a$ increases, while B decreases, so that the machine switches from "saturation limited" to "thermally limited." This statement can be substantiated by observing that in the case $\alpha = 0$, $K_a/B$ varies as $\tan\psi$. The choice of the design value of $\psi$ is dictated by various considerations which will be discussed in the following section.

## 3. Selection of Operating Point

The design of a PM motor today must be based on two possible modes of operation: constant and adjustable frequency. In the case of constant frequency supply, the machine is operated in steady state as a synchronous machine and is brought up to speed by relying on the squirrel-cage winding. In this case the machine must meet the specifications with regard to synchronous pull-in torque and asynchronous starting and pull-out torques, besides rated torque. In the case of adjustable-frequency supply, the machine operates as a "brushless dc motor." In operation as an electronically commutated machine (ECM) with closed loop control of the firing angle of the switching elements, the angle $\psi$ can be maintained at that value for which the delivered torque is maximum. An increase in load torque, then, causes a drop in speed and, hence, in the electromotive force $e_a$. This, in turn, causes the armature current and, hence, the torque to rise, as in a dc machine. In fact the dc machine represents the particular case in which the angle $\psi$, as determined by the brush position, is constant and normally equal to zero.

It should be noted that, whereas iron saturation imposes an absolute limit on the allowable magnetic loading, the maximum electric loading is determined by the thermal considerations and, therefore, depends on the time duty-cycle. As a result, the value of K required to develop the peak torque is not subject to restrictions, because it occurs during a very short time only, at pull-in.

It follows that the design should be based on B. In this regard, however, one must remember that usually PM motors are built with uniform air gaps and, therefore, the field excited by the magnet has a distribution which is approximately rectangular. This departure from a sinusoidal distribution must be taken into account in assessing iron saturation. Therefore, the B which is significant for the design is not the rms value at the gap, but the maximum value at which the teeth are exposed.

Since the mmf of the field and armature are additive towards the tip of the pole, as sketched in Fig. 6, the highest value of B occurs in the teeth facing it. To determine this value, the armature current density $K_a$ is decomposed into its components along the direct and quadrature axes and it is expressed as a function of the linear coordinate x along the periphery of the gap:

$$K_a(x) = K_{ad}(x) + K_{aq}(x)$$

$$= \sqrt{2}\, K_a \left( \sin \frac{2px}{D} \sin |\psi| + \cos \frac{2px}{D} \cos \psi \right) \qquad (14)$$

If the B lines were straight across a uniform gap, the corresponding $B_a$ could be written as

$$B_a(x) = \sqrt{2}\, B_a \left( \frac{a+b}{a+b+ab} \cos \frac{2px}{D} \sin |\psi| + \sin \frac{2px}{D} \cos \psi \right) \qquad (15)$$

where the first term on the right hand side is much smaller than the second term, because the permeance along the d-axis is much smaller than along the g-axis. With this in mind and taking into account the presence of the interpolar space, the flux distribution in the gap of a PM motor can be depicted as sketched in Fig. 7 for one q-axis and one d-axis. It should be noted that such a flux distribution prevails with all kinds of pole and magnet arrangements, even though, for heuristic purposes a salient pole configuration has been shown.

To $B_a$ one must add the field produced by the permanent magnet

$$B_m = \frac{\mu_o}{g} \frac{a}{a+b+ab} F_M = \sqrt{2} \frac{B_f}{C_f} \tag{16}$$

As Figs. 6 and 7 show, B peaks at the leading edge of the pole for $x \sim \ell_p/2$ where $B_{aq}$ approaches the maximum value. If $\ell_{Fe}$ represents the actual length of the lamination stacks, $\tau_s$ the slot pitch, $w_t$ the tooth width, and if one assumes that the slot carries no flux, then it follows from the principle of continuity of flux that the value of B at the tooth which has the highest flux density is

$$B_t = \sqrt{2} \frac{L}{\ell_{Fe}} \frac{\tau_s}{w_t} \left[ B_a \sin \left(\frac{p\ell_p}{D}\right) \cos\psi + \frac{B_f}{C_f} \right] \tag{17}$$

so that

$$B_f = \left[ \frac{B_t}{\sqrt{2}} \frac{\ell_{Fe}}{L} \frac{w_t}{\tau_s} - B_a \sin \left( \frac{p\ell_p}{D} \right) \cos\psi \right] C_f \tag{18}$$

Making use of Eqs. (10) and (7) to eliminate $B_a$, one obtains

$$B_f = \frac{B\cos\alpha}{\cos\psi} - B\,\frac{(C_q - C_d')\sin|\psi|}{C_q}\,\frac{\sin|\psi-\alpha|}{\cos\psi}$$

$$= \left[\frac{B_t}{\sqrt{2}}\,\frac{\ell_{Fe}}{L}\,\frac{w_t}{\tau_s} - B\,\frac{\sin(\frac{p\ell_p}{D})\sin|\psi-\alpha|}{C_q}\right] C_f \tag{19}$$

and solving for B yields

$$B = \frac{\frac{B_t}{\sqrt{2}}\,\frac{\ell_{Fe}}{L}\,\frac{w_t}{\tau_s}\,C_f}{\frac{\cos\alpha}{\cos\psi} - \frac{C_q - C_d'}{C_q}\,\frac{\sin|\psi|\sin|\psi-\alpha|}{\cos\psi} + \frac{C_f}{C_q}\,\sin\left(\frac{p\ell_p}{D}\right)\sin|\psi-\alpha|} \tag{20}$$

The force per unit surface $< f_e >$ of Eq. (9) is then

$$< f_e > = \frac{2p(g/D)}{\mu_o}\,\frac{\sin|\psi-\alpha|}{C_q\cos\psi}\,B^2\cos\alpha$$

$$= \frac{2p(g/D)}{\mu_o}\left(\frac{B_t}{\sqrt{2}}\,\frac{\ell_{Fe}}{L}\,\frac{w_t}{\tau_s}\right)^2\,\frac{C_q}{F(\psi)} \tag{21}$$

where

$$F(\psi) = \frac{\cos\psi\{\sin(\frac{p\ell_p}{D})\sin|\psi-\alpha| + \frac{1}{C_f\cos\psi}[C_q\cos\alpha - (C_q - C_d')\sin|\psi|\sin|\psi-\alpha|]\}^2}{\sin|\psi-\alpha|\cos\alpha} \tag{22}$$

Accordingly, Eq. (9) for the torque becomes

$$T = 2p\left\{\frac{1}{2\mu_o}\left[\frac{\ell_{Fe}}{L}\,\frac{B_t}{\sqrt{2}}\,\frac{w_t}{\tau_s}\right]^2\,(\pi DLg)\right\}\frac{C_q}{F(\psi)} \tag{23}$$

where the term in the large brackets is an index of the energy stored in the gap and is representative of the dimensions of the machine.

Other parameters being equal, the torque increases in proportion to the number of poles.

The general trend of $F(\psi)$ is shown in Fig. 8 where the following parameter values have been used

$$\alpha = 0 \qquad \frac{\ell_p}{\tau} = 0.9 \quad \text{or} \quad \frac{p\ell_p}{D} = 1.413$$

$$C_f = 1.25 \qquad C_d = 1 \qquad C_q = 0.8 \qquad (24)$$

$$C'_d = 0.25$$

It is clear from Eq. (24) that, for given values of $B_t$ and of the other parameters, the operating point should be chosen at a $\psi$ near the minimum of $F(\psi)$, in order to minimize the dimensions of the machine. Since a function does not vary rapidly around the minimum, the strong dependence of $K_a$ on $\psi$ ensures that it is possible to choose a $\psi$ which keeps the electric loading, as well as the magnetic one, within allowable limits, without significant departure from the minimum bore dimensions.

The dependence of the minimal value of $F(\psi)$ and of the corresponding value of $\psi$ on $\alpha$, the pole arc ratio $\ell_p/\tau$, and $C'_d$ is displayed in Table 1.

As could be expected $F(\psi)$ and, therefore, the dimensions of the machine are larger for an overexcited machine, than for an underexcited one. It also appears that the pole arc ratio $\ell_p/\tau$ and, therefore, $C_f$, $C_d$, and $C_q$ which depend on it have no effect on $F(\psi)$ and little effect on $\psi$. This is very fortunate, because the pole arc and its derived quantities cannot be predicted accurately.

Table 1

Minimal $F(\psi)$ and corresponding $\psi$

| | Underexcitation $\alpha = +25°$ | | Overexcitation $\alpha = -25°$ | |
|---|---|---|---|---|
| $\frac{\ell_p}{\tau}$ \ $C'_d$ | 0.25 | 0.40 | 0.25 | 0.40 |
| 0.7 | $f(\psi) = 0.7$<br>$\psi = -76°$ | $F(\psi) = 1.2$<br>$\psi = -72°$ | $F(\psi) = 1.04$<br>$\psi = -80°$ | $F(\psi) = 1.62$<br>$\psi = -72°$ |
| 0.9 | $F(\psi) = 0.7$<br>$\psi = -80°$ | $F(\psi) = 1.2$<br>$\psi = -76°$ | $F(\psi) = 1.04$<br>$\psi = -80°$ | $F(\psi) = 1.62$<br>$\psi = -76°$ |

The reason is that, for the sake of mechanical strength, the poles of PM machines are often connected to one another at the gap by thin bridges which are deliberately driven hard into saturation, as is the case with the bridges closing the slots of squirrel-cage rotors. In contrast, the effective reactance coefficient in the direct axis, $C'_d$, has a strong effect on the minimal value of $F(\psi)$ and some effect on $\psi$. The value $C'_d = 0.25$ corresponds to a ratio of leakage to gap reluctance a = 10 and a ratio of magnet to gap reluctance b = 4. The value $C'_d = 0.4$ corresponds, instead, to a ratio of leakage to gap reluctance a = 5 and a ratio of magnet to gap reluctance b = 2. It follows that accurate prediction of a and b is important.

In the case of permanent magnet machines it is also important to minimize the volume of the magnets because of economy considerations and in order to ensure that the magnets can be accommodated within the rotor.

An equation similar to Eq. (23) can be derived to relate the torque to the volume and energy stored in the permanent magnets.

Let $A_M$ denote the cross-section of the magnet and $\ell_M$ its length. The magnet flux is

$$\Phi_M = A_M B_M = \frac{2}{\pi} L \frac{\pi D}{2p} \sigma \sqrt{2} B_f = \frac{LD}{p} \sigma \sqrt{2} B_f \tag{25}$$

where $\sigma = 1 + \frac{1}{a}$ = flux leakage coefficient.

The length of the magnet is

$$\ell_M = - \frac{2\sqrt{2}}{C_f} \frac{B_f}{\mu_o H_M} g \tag{26}$$

where $H_M$, the magnetic field intensity in the magnet, is negative.

It should be noted that $B_f$, as obtained from Eqs. (25) and (26) in terms of the operating point ($H_M B_M$) of the magnet, is the same as given by Eq. (16) in terms of $F_M$ and, therefore, $H_c$.

It follows from Eqs. (25) and (26) that the volume of one magnet is

$$A_M \ell_M = - \frac{2}{\pi} \frac{(\sqrt{2} B_f)^2}{\frac{\mu_o H_M B_M}{2}} \frac{\sigma \pi DLg}{2p C_f} \tag{27}$$

Introducing the value for $B_f$ from Eq. (19) and making use of Eqs. (21) and (9), the torque can be expressed as:

$$T = p[( - H_M B_M) (p A_M \ell_M)] \frac{1}{G(\psi)} \tag{28}$$

where

$$G(\psi) = \frac{2}{\pi} \frac{\sigma}{C_f} \frac{C_q \cos\psi}{\sin|\psi-\alpha|\cos\alpha} \left( \frac{\sqrt{2}}{\cos\psi} \right)^2 \left\{ \cos\alpha - (C_q - C_d') \frac{\sin|\psi|\sin|\psi-\alpha|}{C_q} \right\}^2 \tag{29}$$

Again with other parameters being the same, the torque increases in proportion to the number of poles. The terms in the square brackets of Eq. (28) represent the energy product times the volume of the magnets. As could be expected, for given torque and energy product the volume of the magnets increases in proportion to the leakage coefficient $\sigma$, because this coefficient affects the width of the magnets directly. For this reason it is expedient to plot $G(\psi)/\sigma$, rather than $G(\psi)$. For the parameters of Eq. (24) $G(\psi)/\sigma$ is shown in Fig. 9.

As could also be expected, for given torque and energy product, the volume of the magnets is inversely proportional to $C_f$ because this coefficient affects the length of the magnets directly. $C_f$, however, as well as $C_q$ and $C_d$ are functions of the pole arc ratio $\ell_p/\tau$. The dependence of the minimal value of $G(\psi)/\sigma$ and of the corresponding value of $\psi$ on $\alpha$, $\ell_p/\tau$, and $C_d'$ is displayed in Table 2.

It is seen that the pole arc ratio has a stronger influence on $G(\psi)$, than on $F(\psi)$. The effects of $\alpha$ and $C_d'$ on $G(\psi)$ and $F(\psi)$ have similar trends.

In order to minimize the volume of the magnets, the operating point should be chosen at a value of $\psi$ near the minimum of $G(\psi)$. Fortunately the minima of $F(\psi)$ and $G(\psi)$ occur in the same neighborhood around $|\psi| = 70°$.

The finding that the optimal $\psi$ for maximum torque demand lies in the neighborhood of 70° allows to select B in conformity with Eq. (20).

These choices of $\psi$ and B, in turn uniquely determine the surface current density $K_{aR}$ which according to Eq. (10) is

$$K_{aR} = \frac{2p}{\mu_o}\left(\frac{g}{D}\right)\frac{\sin|\psi-\alpha|}{C_q \cos\psi}\ B \qquad (30)$$

Table 2

Minimal $\frac{G(\psi)}{\sigma}$ and corresponding $\psi$

| | Underexcitation $\alpha = +25°$ | | Overexcitation $\alpha = -25°$ | |
|---|---|---|---|---|
| $\frac{\ell_p}{\tau}$ \ $C'_d$ | 0.25 | 0.40 | 0.25 | 0.40 |
| 0.7 | $\frac{G(\psi)}{\sigma} = 0.21$<br>$\psi = -64°$ | $\frac{G(\psi)}{\sigma} = 0.48$<br>$\psi = -52°$ | $\frac{G(\psi)}{\sigma} = 0.81$<br>$\psi = -72°$ | $\frac{G(\psi)}{\sigma} = 1.37$<br>$\psi = -68°$ |
| 0.9 | $\frac{G(\psi)}{\sigma} = 0.17$<br>$\psi = -64°$ | $\frac{G(\psi)}{\sigma} = 0.4$<br>$\psi = -56°$ | $\frac{G(\psi)}{\sigma} = 0.72$<br>$\psi = -76°$ | $\frac{G(\psi)}{\sigma} = 1.22$<br>$\psi = -68°$ |

## 4. Design Guidelines

The design of the motor is accomplished in two steps. The first step consists of the determination of the main dimensions directly from the performance specifications.

The second step consists of flux mappings by means such as the finite elements analysis and, if needed, suggests refinements in the geometries of the slots and magnets. This step yields values of the

saturated inductances, developed torque, and stresses on the teeth, values that are used to verify the original assumptions.

The bore dimensions are determined by thermal considerations which involve the steady-state or effective copper loss in the winding, its allowable temperature rise, and an empirical heat transfer coefficient[3]. In the case of PM motors the sensitivity of the magnets to temperature imposes an additional limitation on the temperature rise, besides the one imposed by the class of insulation. The temperature should not be allowed to rise more than 70°C above the 40°C ambient and, therefore the use of insulation of higher class than F is not warranted.

As a first guess one may assume[3]

$$D = 0.0189\ P_i^{0.29}\ p^{0.55}\ f^{-0.23} \tag{31}$$

where $P_i$ is an ideal power equal to the rated power divided by the product of efficiency and power factor, and

$$L = 0.0297\ P_i^{0.29}\ p^{-0.117}\ f^{-0.23} \tag{32}$$

Next one calculates the values of $\psi$ which minimize $F(\psi)$ of Eq. (22) and $G(\phi)$ of Eq. (29) with assumed values $C_d'$, $C_q$, and $C_f$. These values of $\psi$ give the optimal operating point for given bore dimensions and magnet volume respectively.

The ratio of the effective gap length to the bore diameter is determined by mechanical considerations which lead to

$$\frac{g}{D} \sim 10^{-2}\ P_i^{0.01}\ p^{-0.5} \tag{33}$$

Introducing g from this equation and the minimum value of $\psi$ previously obtained into Eq. (23) gives the flux density $B_t$ in the most stressed tooth. If $B_t$ exceeds the limited value dictated by saturation (2.1T), then one must increase the tooth with $w_t$ or the bore dimensions.

The surface current density $K_a$ and the effective flux density B are calculated from Eqs. (11) and (12), introducing $\langle f_e \rangle$ from Eq. (9). The field flux density $B_f$ is, then, given by Eq. (19).

Next one must determine the geometry of the magnets from Eqs. (25) and (26). A word of caution is in order at this point. The volume of the magnets is sensitively dependent on the assumed values of the parameters. Of these a and $\sigma$, which are indexes of the reluctance of the leakage paths around the magnets, depend on the saturation and, hence, vary with the operating point. For these reasons, in the final design it is essential to confirm the assumptions made, by performing mapping of the flux for various conditions of operation.

When magnets having the dimensions given by Eqs. (25) and (26) cannot be accommodated within the rotor, there are two possibilities:

a) If $\psi$ is larger than the value which minimizes $G(\psi)$, then $\psi$ can be reduced.

b) If $\psi$ is equal or smaller than the value which minimizes $G(\psi)$, then the bore dimensions must be increased.

Only a few iterations are needed in order to converge to the final result.

The number of turns per phase is given by Eq. (5).

This completes the basic design for a motor which is operated as a brushless dc machine. If the machine is designed to operate also with a constant frequency, constant voltage supply, a smaller value of $\psi$, then the optimal one should be selected. A reduction of about ten degrees should allow to pull-in at rated torque with reasonable load inertia. A lower $\psi$ also leads according to Eq. (11) and (12) to a smaller $K_a/B$ ratio. This reduces the value of the leakage impedances and increases the starting and pull-out torques with asynchronous operation.

## 6. Space Requirements

At present, the size of the permanent magnets and, therefore, the power level of a PM motor is limited by manufacturing difficulties and costs. There exists, however, another limitation which stems from the basic difference between the space requirements of current and PM excitations.

The space required for current excitation is independent of the pole face length $\ell_p$ and, hence, of the pole pitch $\tau$. In contrast, in the case of PM excitation, this space depends on $\tau$, because the cross section of the magnet must carry the flux. The two situations are compared in Fig. 10. To ease the comparison, this is made for a flux concentrator type of magnet arrangement. The results, however, are quite general, because as Eq. (27) shows the volume of the magnets is independent of the arrangement.

The mmf per pole pair in the case of current excitation is obtained replacing $(-H_M \ell_m)$ of Eq. (26) by $2N_f I_f$ where $N_f$ is the number of field turns per pole and $I_f$ is the field current. The result is

$$2N_f I_f = 2\,\frac{\sqrt{2}\,B_f g}{\mu_o C_f} \tag{34}$$

The space required for the winding can be found by introducing the volume current density $J_f$ and a copper filling factor $k_{Cu}$ defined as the ratio of the cross section of the copper to the total cross section $A_f$ of the winding. Introducing

$$2N_f I_f = k_{Cu}\, J_f\, A_f \tag{35}$$

into Eq. (34) and solving for $A_f$ one obtains

$$A_f = \frac{2\sqrt{2}\,B_f g}{\mu_o C_f}\;\frac{1}{J_f k_{Cu}} \tag{36}$$

The corresponding cross section in the case of PM excitation is, according to Eq. (27)

$$\frac{A_M \ell_M}{L} = \frac{2\sqrt{2}\,B_f g}{\mu_o C_f}\,\frac{\sqrt{2}\,B_f \sigma D}{(-H_M B_M)2p} = \frac{2\sqrt{2}\,B_f g}{\mu_o C_f}\left[\frac{\sqrt{2}}{\pi}\;\frac{\sigma\tau B_f}{(-H_M B_M)}\right] \tag{37}$$

comparison between Eqs. (36) and (37) shows that PM excitation will require a larger share of the rotor cross section when

$$\tau > \frac{\pi}{\sqrt{2}}\;\frac{-H_M B_M}{2}\;\frac{1}{B_f \sigma J_f k_{Cu}} \tag{38}$$

Taking, for instance, the typical values $B_M = 0.4T$; $B_f = 0.6T$; $\sigma = 1.1$; $J_f = 5 \times 10^6\ \frac{A}{m^2}$ i $k_{Cu} = 0.5$ one finds that $\tau$ should not exceed 0.086m. This severely limits the power level of PM motors, especially when the number of poles is small.

Acknowledgment

Part of the work reported in this paper was taken from the dissertation of A. Levran, submitted to the faculty of the Polytechnic Institute of New York in partial fulfillment of the requirements for a Ph.D. Degree in 1983. This work was also supported in part by the U.S. Department of Transportation under Contracts Nos. DOT-FR-64227 and DTRS5681-C-00023.

References

1. D.J. Hanrahan, and D.S. Toffolo, "Permanent Magnet Generators, Part I, Theory" AIEE Trans. Vol. 76 Part III, pp. 1098-1103, 1957.
2. V.W. Volkrodt, "Polradspannung, Reactanzen and Ortscurve des Stromes der mit Dauermagneten erregten Synchronmachine," ETZ, pp. 517-522, 1962.
3. E. Levi, Polyphase Motors: A Direct Approach to their Design, John Wiley, New York, 1983.

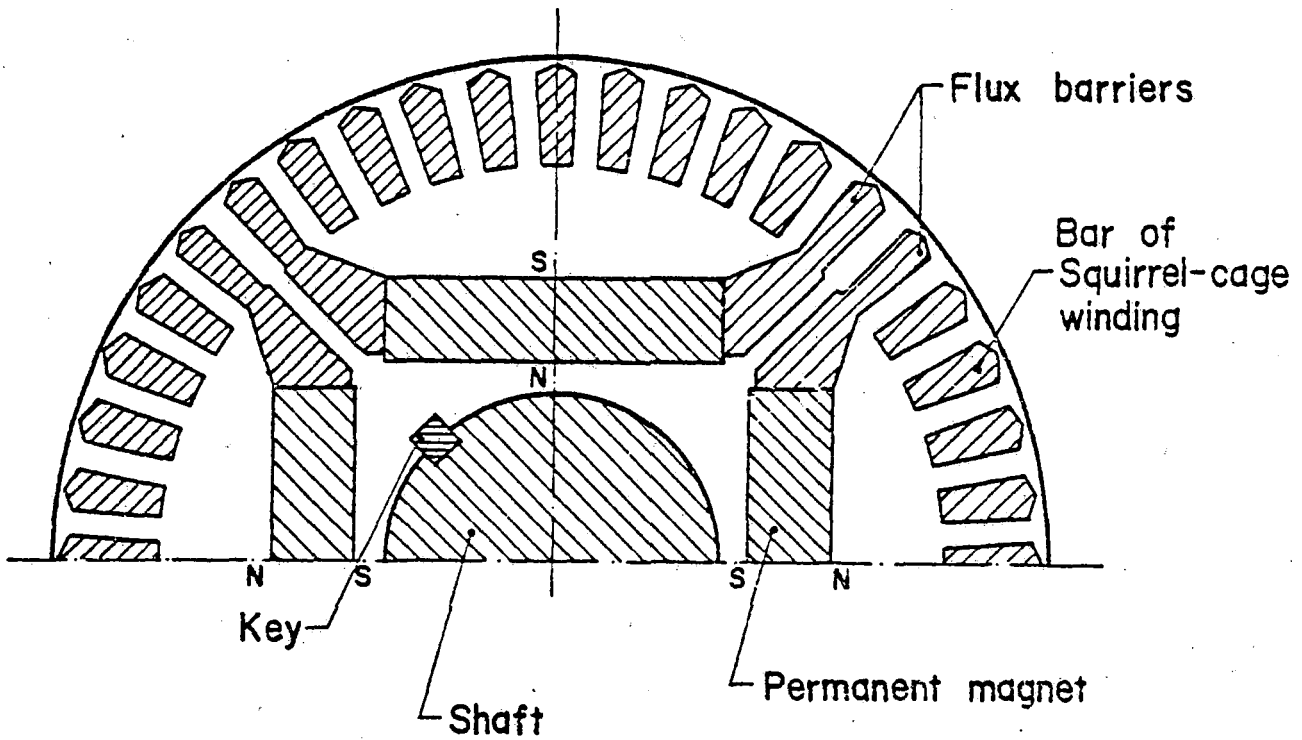


Fig. 1. Cross section of rotor of PM motor (from: C. Steen, U.S. Patent No. 4,137,790, Feb. 13, 1979).

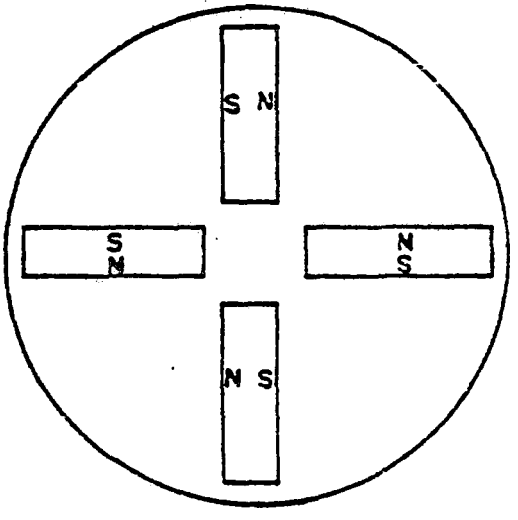


Fig. 2. Flux concentration arrangement of permanent magnets.

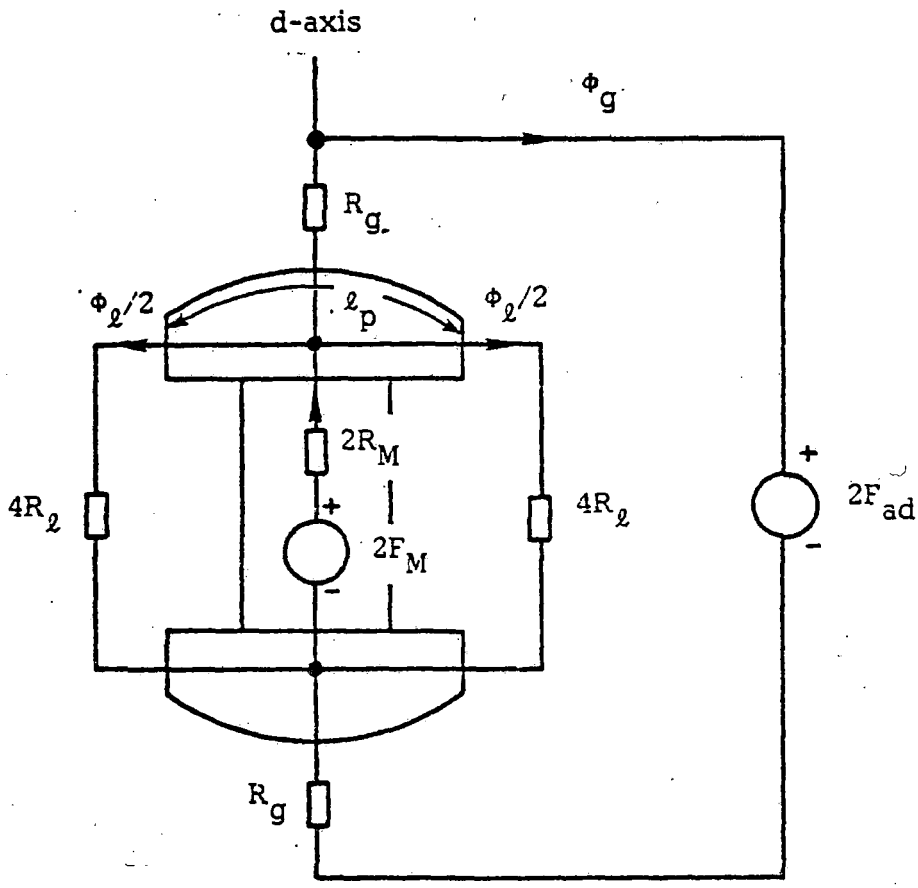


Fig. 3. Magnetic circuit in the direct axis of PM machine.

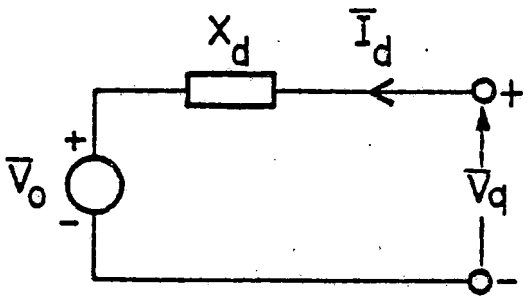


Fig. 4. Thevenin equivalent circuit.

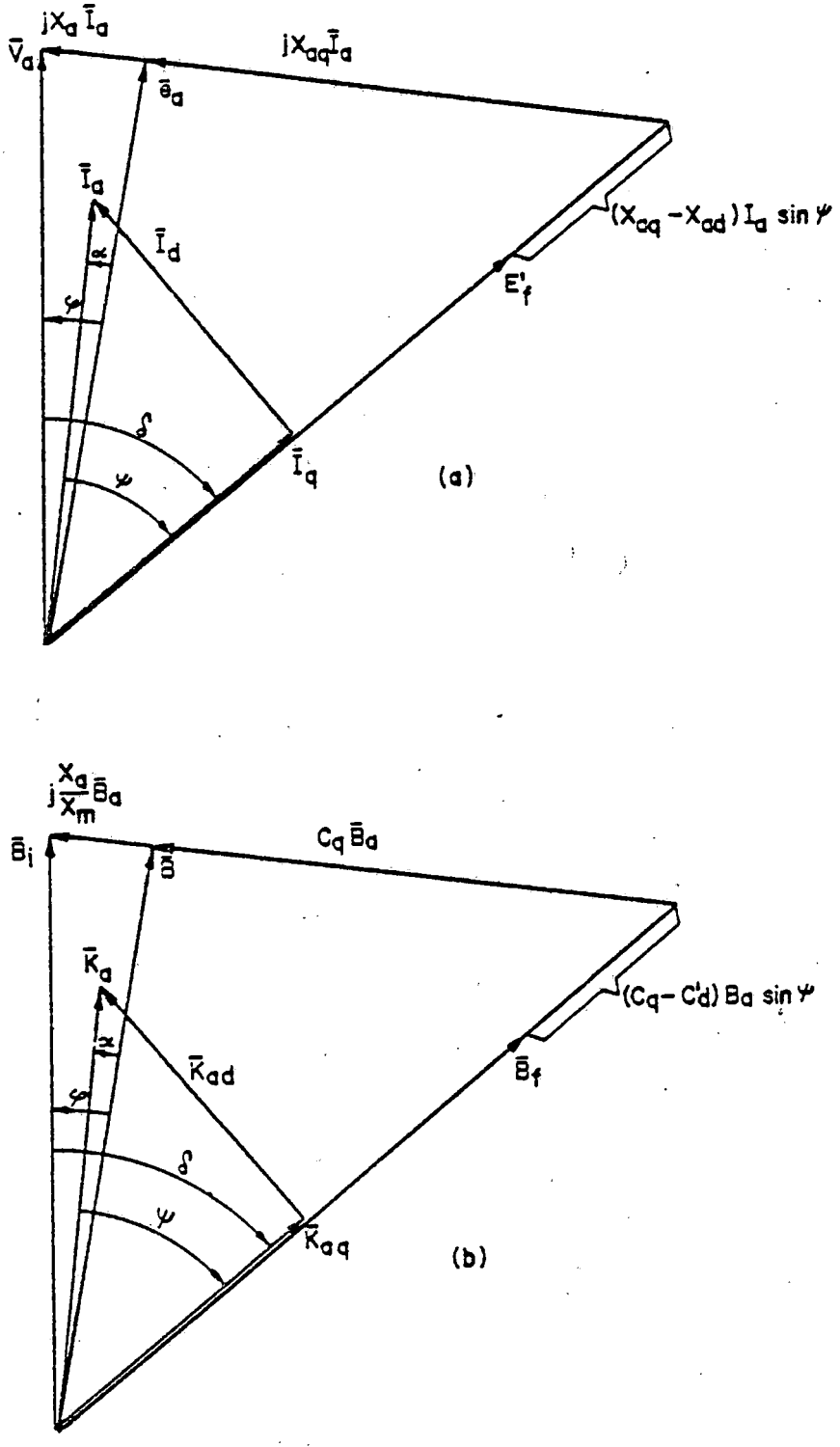


Fig. 5. Phasor diagram of PM machine: (a) terminal quantities, (b) field quantities.

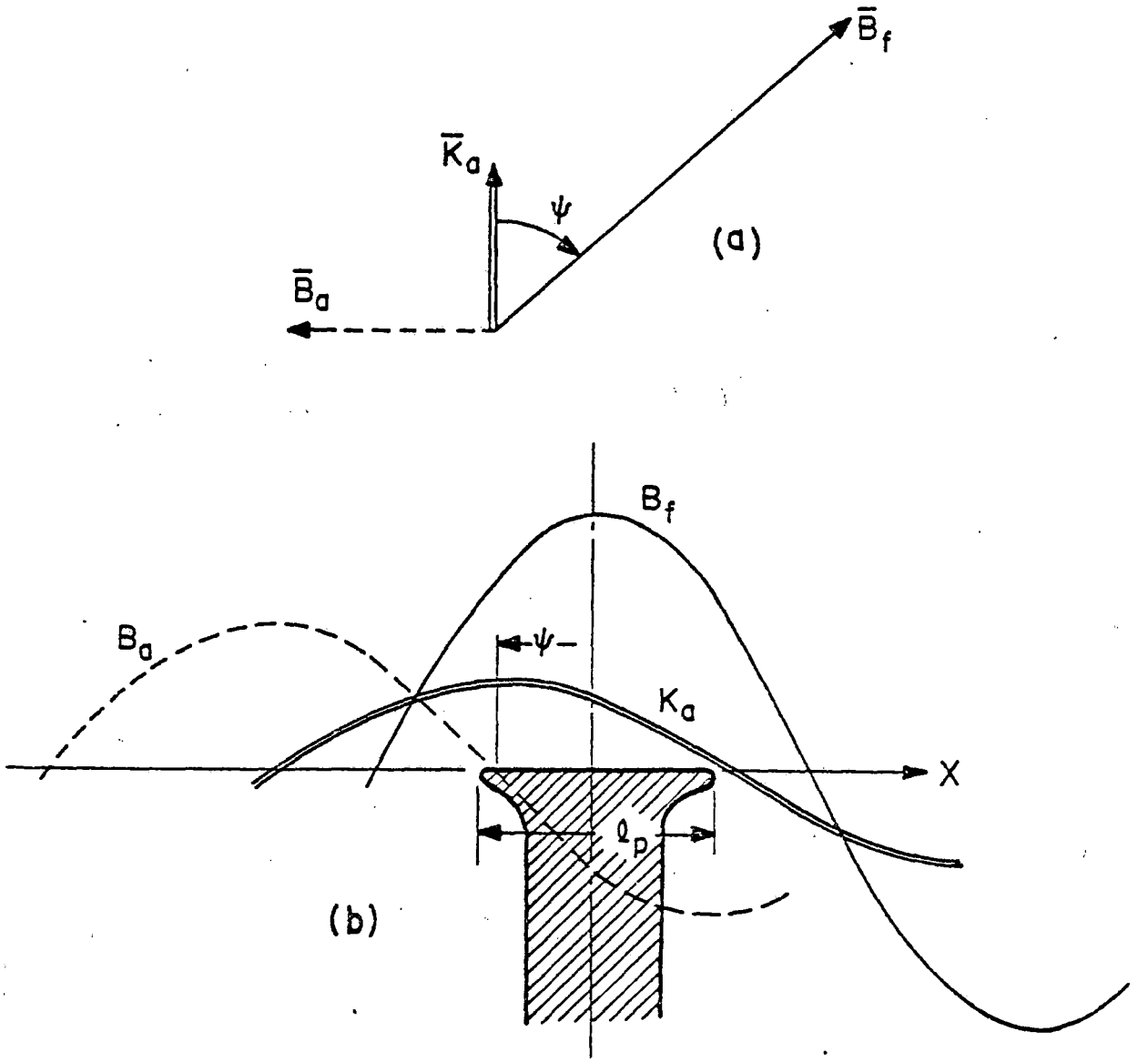


Fig. 6. Relation between fundamental component of armature and field-produced B: (a) phasor diagram, (b) flux distribution.

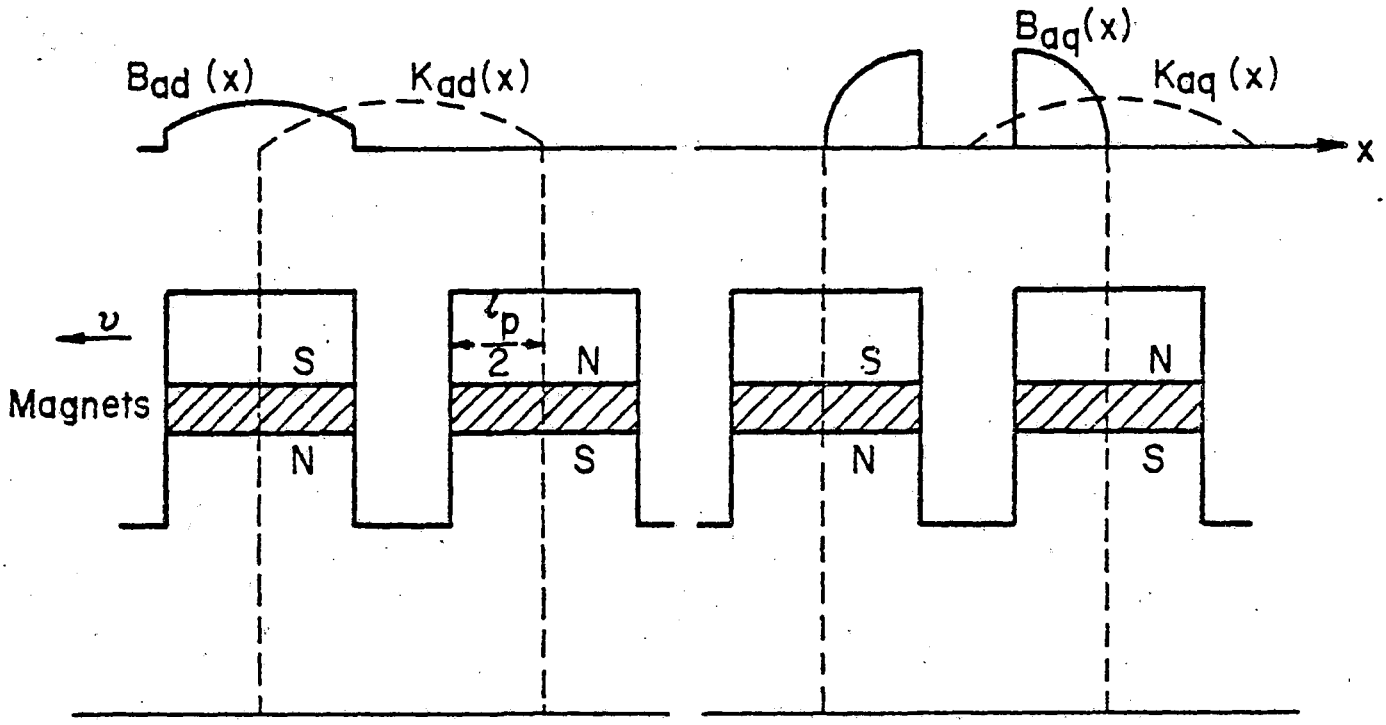


Fig. 7. Magnetic flux distribution in the gap of a PM motor.

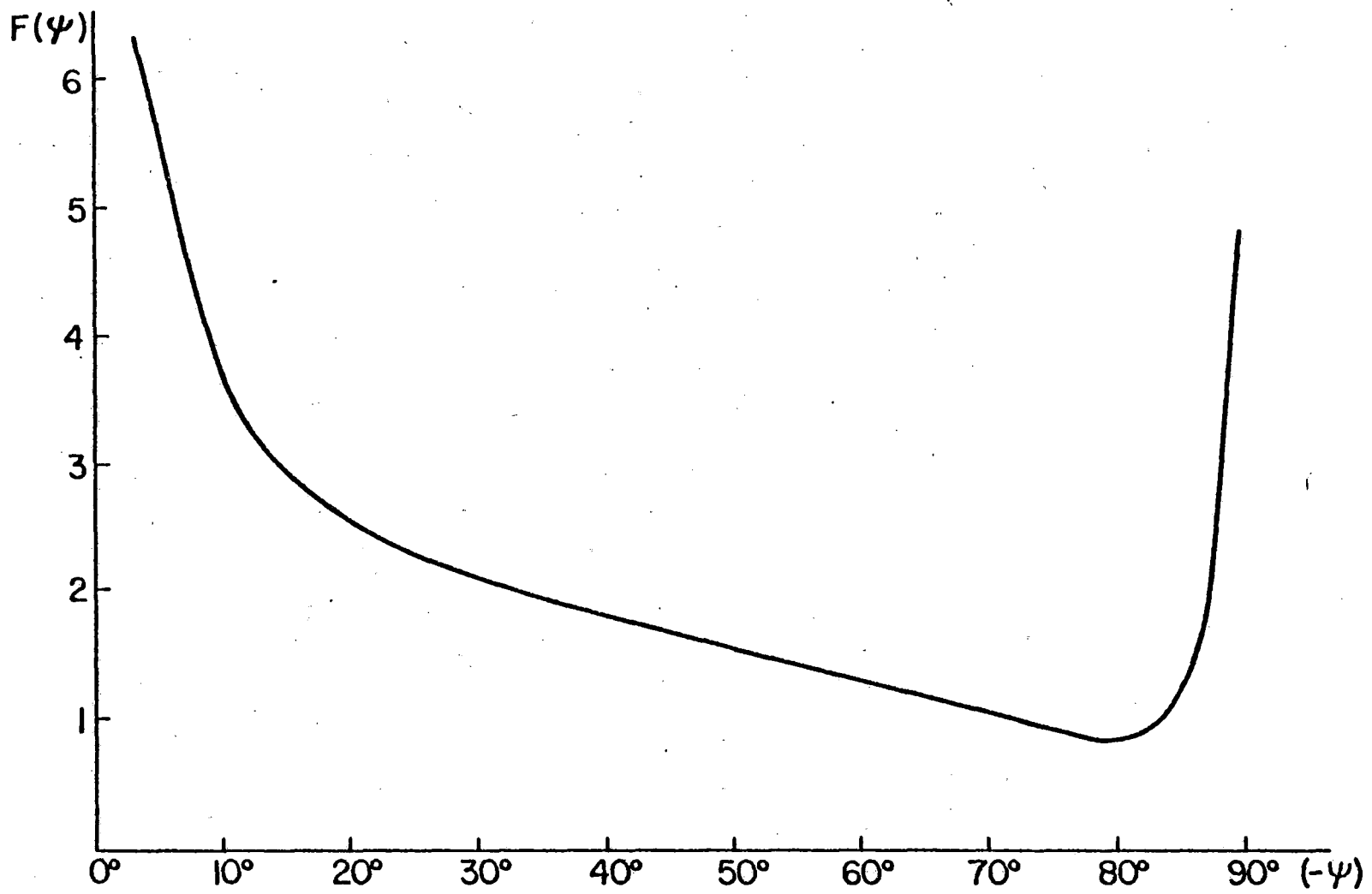


Fig. 8. Plot of $F(\psi)$ vs. $(-\psi)$. $\alpha = 0$, $\ell_p/\tau = 0.9$, $C_f = 1.25$, $C_d = 1$, $C_q = 0.8$, $C_d' = 0.25$.

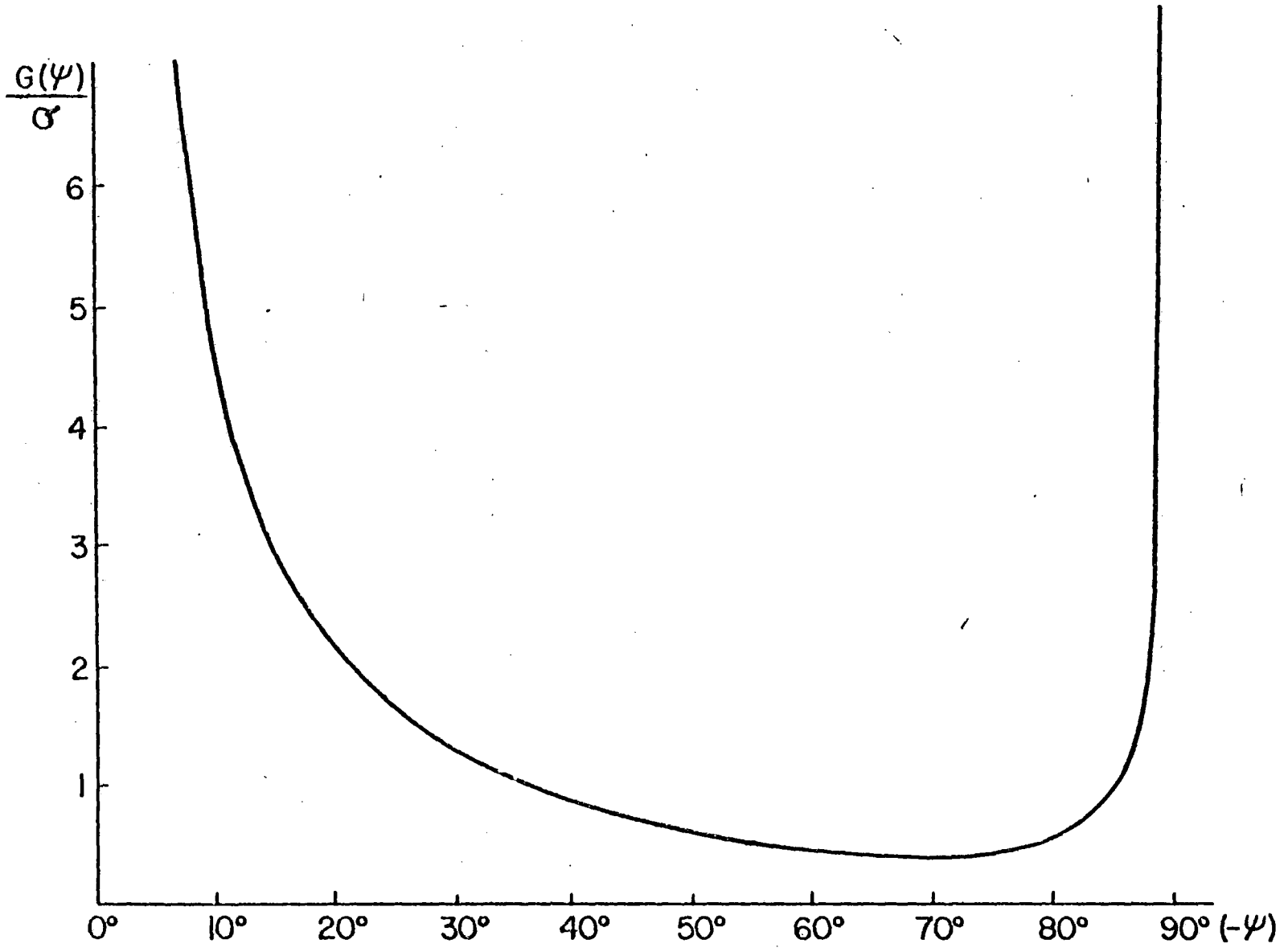


Fig. 9. Plot of $G(\psi)/\sigma$ vs. $(-\psi)$ for the same parameters as in Fig. 8.

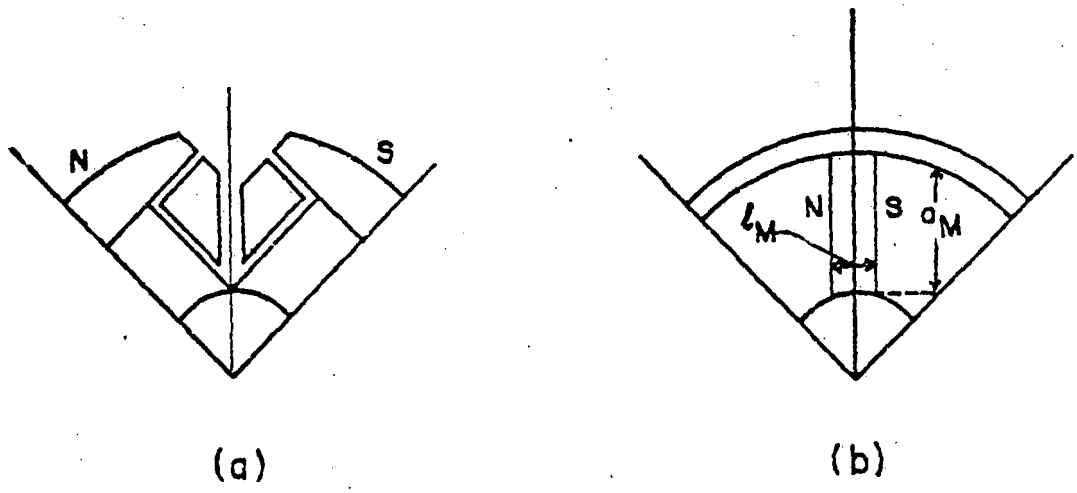


Fig. 10. Cross section of one pitch in rotor of synchronous machine: (a) current excited, (b) PM excited.

## List of Captions

Fig. 1. Cross section of rotor of PM motor (from: C. Steen, U.S. Patent No. 4,137,790, Feb. 13, 1979).

Fig. 2. Flux concentration arrangement of permanent magnets.

Fig. 3. Magnetic circuit in the direct axis of PM machine.

Fig. 4. Thevenin equivalent circuit.

Fig. 5. Phasor diagram of PM machine: (a) terminal quantities, (b) field quantities.

Fig. 6. Relation between fundamental component of armature and field-produced B: (a) phasor diagram, (b) flux distribution.

Fig. 7. Magnetic flux distribution in the gap of a PM motor.

Fig. 8. Plot of $F(\psi)$ vs. $(-\psi)$. $\alpha = 0$, $\ell_p/\tau = 0.9$, $C_f = 1.25$, $C_d = 1$, $C_q = 0.8$, $C'_d = 0.25$.

Fig. 9. Plot of $G(\psi)/\sigma$ vs. $(-\psi)$ for the same parameters as in Fig. 8.

Fig. 10. Cross section of one pitch in rotor of synchronous machine: (a) current excited, (b) PM excited.

Appendix IV

## APPENDIX IV

### 1. Determination of the Tractive Effort

The starting point for the calculation is the profile of the allowable speed along the track. The profile for the New York to Washington, D.C. segment of the U.S. Northeast Corridor, as shown in Table 1, is chosen for this example. This profile is characterized by the maximum permissible speed of 120 mph (53.76 m/s) on the straight portions of the track and is practically all on level ground. From the allowable speed profile one can derive a speed vs. time curve by assuming appropriate acceleration and deceleration rates. In this case of intercity travel, when the stops are spaced widely apart, the acceleration rate can remain well below the maximum allowable acceleration for passenger comfort and the limit imposed by the adhesion coefficient. These are around 1.5 $m/s^2$.

In view of the fact that the resistance to motion increases as the square of the speed, and in order to keep the power requirements within bounds, the acceleration should decrease with increasing speed. Assuming that the acceleration decays exponentially from a starting value of 0.5 $m/s^2$ to a value of 0.05 $m/s^2$ at the maximum speed of 120 mph, one obtains

$$a = 0.5 \exp [- 0.00837 t]$$

Similar considerations lead to a deceleration rate

$$a = - 0.5 \exp [0.05 t]$$

The corresponding speed vs. time curve is sketched in Fig. 1. The intervals at zero speed correspond to five intermediate stops. This profile must be combined with the relation of the tractive effort vs. speed in order to obtain the tractive effort vs. time.

TABLE 1

AMT-1 SPEED TABLE NEW YORK TO WASHINGTON, D.C.

| FROM MILEPOST | TO MILEPOST | SPEED LIMIT | FROM MILEPOST | TO MILEPOST | SPEED LIMIT |
|---|---|---|---|---|---|
| 0 | 0.72 | 15. | 6.90 | 7.34 | 82. |
| 0.72 | 3.01 | 60. | 7.34 | 9.32 | 120. |
| 3.01 | 3.69 | 84. | 9.32 | 11.16 | 113. |
| 3.69 | 8.06 | 100. | 11.16 | 17.85 | 120. |
| 8.06 | 8.40 | 60. | 17.85 | 19.94 | 113. |
| 8.40 | 9.00 | 45. | 19.94 | 21.81 | 120. |
| 9.00 | 9.35 | 77. | 21.81 | 22.83 | 101. |
| 9.35 | 10.66 | 113. | 22.83 | 23.90 | 98. |
| 10.66 | 13.95 | 120. | 23.90 | 26.09 | 120. |
| 13.95 | 14.80 | 81. | 26.09 | 26.90 | 55. |
| 14.80 | 20.35 | 120. | 26.90 | 27.62 | 58. |
| 20.35 | 20.89 | 105. | 27.62 | 29.97 | 120. |
| 20.89 | 21.80 | 116. | 29.97 | 30.50 | 113. |
| 21.80 | 22.14 | 111. | 30.50 | 59.40 | 120. |
| 22.14 | 23.58 | 120. | 59.40 | 60.80 | 105. |
| 23.58 | 24.05 | 98. | 60.80 | 64.53 | 120. |
| 24.05 | 24.68 | 93. | 64.53 | 65.52 | 113. |
| 24.68 | 26.30 | 105. | 65.52 | 71.92 | 120. |
| 26.30 | 26.75 | 80. | 71.92 | 72.50 | 105. |
| 26.75 | 27.28 | 93. | 72.50 | 77.69 | 120. |
| 27.28 | 27.79 | 118. | 77.69 | 78.49 | 101. |
| 27.79 | 56.15 | 120. | 78.49 | 79.50 | 105. |
| 56.15 | 56.85 | 45. | 79.50 | 86.48 | 120. |
| 56.85 | 74.55 | 120. | 86.48 | 88.29 | 118. |
| 74.55 | 75.18 | 113. | 88.29 | 91.77 | 120. |
| 75.18 | 80.81 | 120. | 91.77 | 91.89 | 69. |
| 80.81 | 81.29 | 84. | 91.89 | 92.54 | 65. |
| 81.29 | 81.88 | 52. | 92.54 | 93.75 | 79. |
| 81.88 | 83.46 | 120 | 93.75 | 94.10 | 57. |
| 83.46 | 84.74 | 72. | 94.10 | 95.17 | 45. |
| 84.74 | 85.15 | 50. | 95.17 | 95.70 | 30. |
| 85.15 | 85.57 | 71. | 95.70 | 96.10 | 15. |
| 85.57 | 87.13 | 78. | 96.10 | 96.86 | 44. |
| 87.13 | 1.87 | 30. | 96.86 | 97.20 | 41. |
| 1.87 | 2.12 | 51. | 97.20 | 98.11 | 42. |
| 2.12 | 2.91 | 59. | 98.11 | 98.71 | 64. |
| 2.91 | 3.08 | 70. | 98.71 | 100.09 | 97. |
| 3.08 | 5.30 | 120. | 100.09 | 134.70 | 120. |
| 5.30 | 6.90 | 79. | 134.70 | 135.00 | 44. |
| | | | 135.00 | 135.85 | 15. |

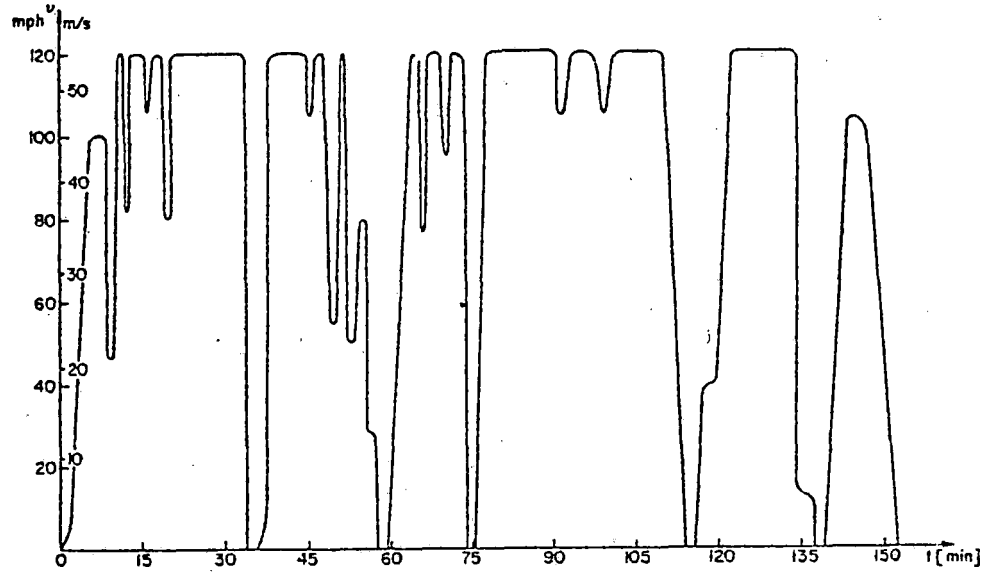


Fig. 1 Profile of train speed vs. time.

The resistance to motion is calculated by using the Davis formulas

For the locomotive

$$R_L = 6.376 \times 10^{-3} m_L + 129n + 3.284 \times 10^{-4} v m_L + 0.572 A v^2$$

For freight cars

$$R_W = 6.376 \times 10^{-3} m_W + 129n + 4.926 \times 10^{-4} v m_W + 0.119 A v^2$$

For passenger cars

$$R_W = 6.376 \times 10^{-3} m_W + 129n + 3.284 \times 10^{-4} v m_W + 0.081 A v^2$$

where m = mass

n = number of axles per car

v = velocity

A = frontal area

and all quantities are expressed in S.I. units.

The train consist includes one 188 tonne (130 tons) locomotive with four driven axles and eight 45 tonne (50 tons) cars. The cross sectional area is A = 11.16 $m^2$ (120 ft.)$^2$. To this one must add the curve resistance given by the equation

$$R_C = \frac{1.1vm}{R}$$

where R is the radius of curvature, to obtain the plots of Fig. 2.

One must still add the acceleration resistances (the grade has been assumed to be zero) in order to calculate the tractive effort T.E. required at each milepost and at each interval of time, as sketched in Fig. 3. Not shown in this table is the negative tractive effort required for braking. The tractive effort peaks at 283 kN at starting and settles down to 113 kN at top speed.

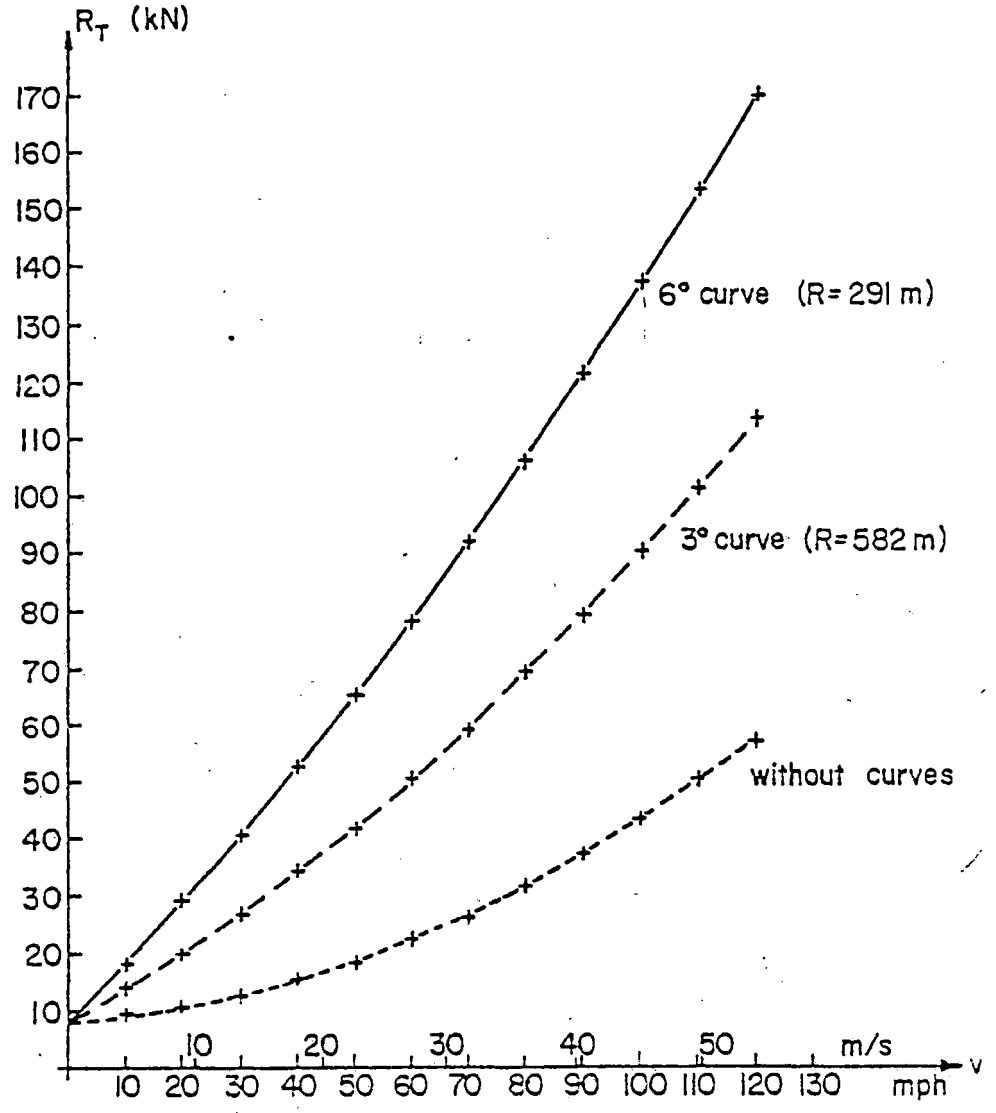


Fig. 2 Train resistance as a function of speed for one locomotive and eight cars.

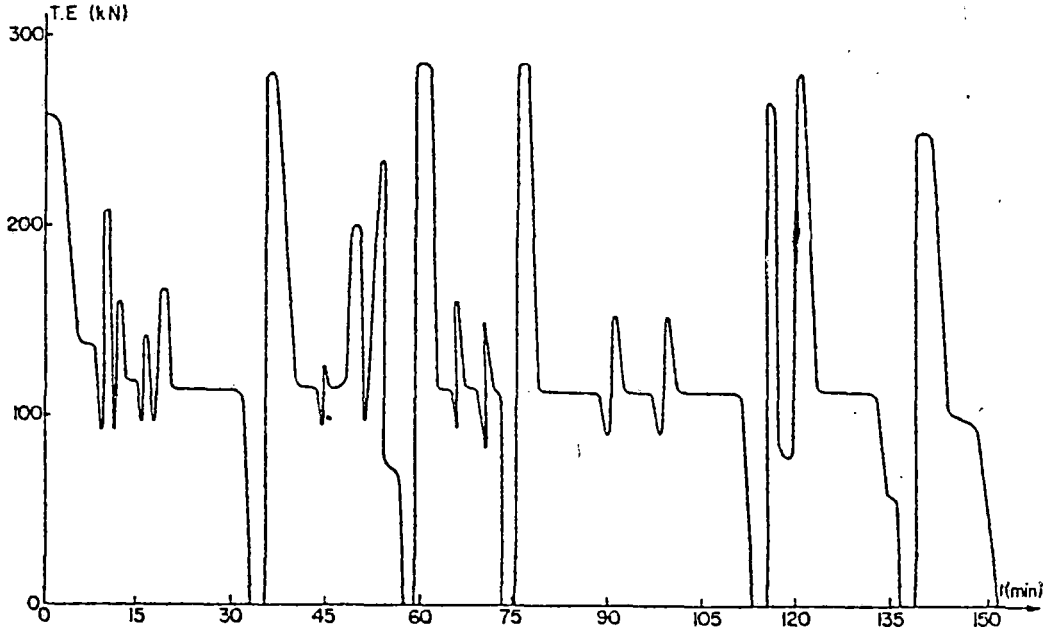


Fig. 3 Profile of the tractive effort vs. time

2. Determination of the Continuous Rating

The motive power can be calculated from the tractive effort as

$$P = \frac{T.E.\times v}{\eta_g}$$

where $\eta_g$, the gear efficiency, is assumed to be 0.97. Since the chosen locomotive has four driven axles and therefore four motors, the power per motor is

$$P_1 = \frac{P}{4}$$

To reach an estimate of the temperature rise in the primary, one has to determine its losses. As a first approximation one may assume that the copper losses are proportional to the delivered power. This in effect is equivalent to the justifiable assumption that the motor, if of the induction type, is operated at constant slip and that the contribution of the magnetization requirements to the rms value of the primary current is negligible.

As a working assumption it is estimated that the copper losses in the primary winding amount to 1.2 percent of the developed power. The calculation of the power required from each motor at each section of the track and of the copper loss in its primary winding, then, shows that a maximum power of 1568kW is needed and that the corresponding loss is 18.8kW.

The temperature rise $\vartheta$ is given by

$$\vartheta = \vartheta_s(1 - e^{-t/\tau_T}) + \vartheta_o e^{-t/\tau_T}$$

where $\vartheta_s$ = steady state temperature rise

$\tau_T$ = thermal time constant.

Under the assumption that $\vartheta_s$ = 130K for maximum power and that $\tau_T$ = 18 min. and using the temperature rise equation for each section of the track one obtains the temperature rise profile shown in Fig. 4. It should be noted that the IEEE Standard for rotating Electric Machinery for Rail and Road Vehicles IEEE Std. 11-1980 allows a temperature rise of 140K with Class F insulation in the stationary winding.

It is interesting to note that, because of the different sequence of the stations, the peak temperature rise in the northbound trip is five percent higher.

From Fig. 4 one can see that the temperature rise during the trip does not exceed 125K. Since the temperature rise of the motor, if operated continuously at the peak power level of 1568KW would be 130K, the equivalent continuous rating is

$$P_R = \frac{125}{130} \times 1568 \sim 1500 \text{ KW}$$

3. Determination of the Basic Parameters of the Motor

The wheel diameter is $D_w$ = 50 in. = 1.27m, and the gear ratio is r = 4. Allowing for a maximum train speed of 130 mph (58.14 m/s), the motor must be designed for

$$n_{max} = 60 \frac{rv}{\pi D_r} = 60 \times 4 \times \frac{58.14}{\pi \times 1.27} = 3500 \text{ rpm.}$$

At 120 mph, this corresponds to

$$n = \frac{120}{130} \times 3500 = 3230 \text{ rpm}$$

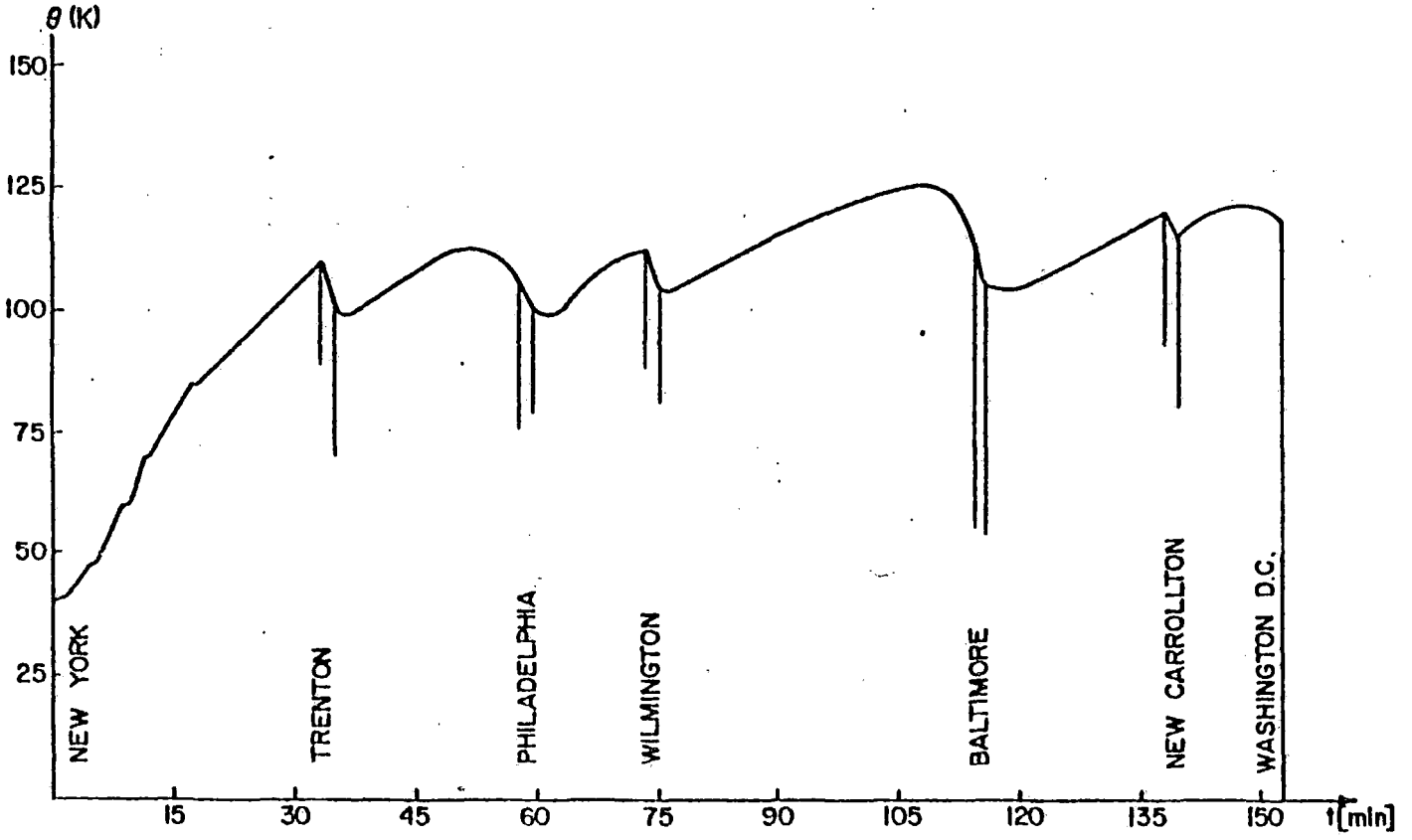


Fig. 4 Profile of temperature rise for an eight car train southbound from New York to Washington

If the number of pole pairs is p = 2, and a 2 percent slip is assumed, the primary frequency peaks at

$$f = \frac{1}{1-0.02} \frac{3230}{60/2} = 109.8 \text{ Hz}$$

In this particular application the bore dimensions are imposed by the space available for mounting the motors on the trucks. This limits the overall length of the motors to 0.88 m and the overall diameter to 0.88 m.

Allowing 2.5cm for the thickness of the housing, one obtains

$$D_o = 0.88 - 2 \times 2.5 \times 10^{-2} = 0.83 \text{ m}$$

Assuming that

$$D_o \sim (1.1 + \frac{0.8}{p}) D$$

one obtains a bore diameter

$$D \sim \frac{0.83}{1.1 + 0.8/2} = 0.55 \text{ m.}$$

The diameter is chosen to be slightly smaller

$$D = 0.52 \text{ m.}$$

The length required in order to accommodate the end windings can be calculated with the help of the following equation

$$\ell_{ew} \sim 2\ell^{(1)} + 2\ell^{(2)} + 2\ell^{(3)}$$

where

$$\ell^{(1)} = \sim 6 \times 10^{-4} V_{ph}^{0.541} \text{ [m]}$$

$$\ell^{(2)} = \frac{y \tau_{s\ ave}(w_s + d)}{2\sqrt{\tau_{s\ ave}^2 - (w_s + d)^2}}$$

$w_s$ = slot width

$y$ = coil span in slot pitches

$d$ = distance between two adjacent coils = $(2.4 + 4.5 \times 1^{-4} V_{ph})10^{-3}$ [m]

$\tau_{save}$ = average slot pitch

$\ell^{(3)}$ = $h_s/2$ + radius of hairpin bend

If the number of stator slots is $Q_1 = 72$, then the slot pitch is

$$\tau_s = \frac{\pi \times 0.52}{72} = 0.0227 \text{ m.}$$

and assuming $w_s/\tau_s = 1/2$, the slot width is

$$w_s = 0.0114 \text{ m.}$$

If $V_{ph} = 1200$ V, the space between two adjacent coils is

$$d \sim (2.4 + 4.5 \times 10^{-4} \times 1200)10^{-3} \sim 3 \times 10^{-3} \text{ m}$$

Letting $\tau_{save} = 1.1\ \tau_s$ and $w/\tau = 2/3$, one obtains for the slanted portion of the end windings

$$2\ell^{(2)} = \frac{(\frac{72 \times 2}{4 \times 3})\ (1.1 \times 2.27)\ (1.14 + 0.3)}{\sqrt{(1.1 \times 2.27)^2 - (1.14 + 0.3)^2}} = 21.15 \text{ cm}$$

The length of the straight portions abutting the slots is

$$2\ell^{(1)} = 2 \times 6 \times 10^{2} \times 1200^{0.541} = 5.6 \text{ cm}$$

and the length needed for the hairpin bends is assumed to be

$$2\ell^{(3)} = 7 \text{ cm.}$$

Allowing 2 cm on each side between the end windings and the end bells the net length available for the lamination stack is

$$L = 0.88 - (2 \times 2.5 + 21.15 + 5.6 + 7 + 2 \times 2) \times 10^{-2} = 0.45 \text{ m}$$

The aspect ratio is then

$$\frac{L}{D} = \frac{0.45}{0.52} = 0.866$$

The bore dimensions being so determined the thermal stress can be ascertained from

$$P_{s\text{-diss}} = \frac{P_{cu}(L/\ell_{co}}{\pi DL} = h\vartheta$$

where $P_{cu} \sim 0.42\ P_i^{0.75}$ = primary copper loss

$P_i \sim 1.1\ P_R^{0.96}\ p^{0.1}\ f^{0.12}$ = ideal power

$\ell_{co} = 1 + \frac{2D}{pL}$ = average length of conductor

$h$ = heat transfer coefficient

The relative length of the conductor is then

$$\frac{\ell_{co}}{L} = 1 + \frac{2}{2}\ \frac{1}{0.866} = 2.155$$

and the ideal power is

$$P_i \sim 1.11(1500000)^{0.96}\ 2^{0.1}(109.8)^{0.12} = 1.77 \times 10^6 W$$

The corresponding loss in the primary winding is

$$P_{cu} = 0.42 \times (1.77 \times 10^6)^{0.75} = 20381W$$

The power dissipated per unit surface is then

$$p_{s\text{-}diss} = h\theta = \frac{20381}{2.155 \times \pi \times 0.52 \times 0.45} = 12865\ Wm^{-2}$$

With the assumed temperature rise $\vartheta$ = 125K, the heat transfer coefficient would be

$$h = \frac{12865}{125} = 102.9\ WK^{-1}m^{-2}$$

This is slightly higher than the value $90WK^{-1}m^{-2}$ usually associated with forced draft ventilation. It should also be noted that the copper loss $P_{cu}$ used here is higher than the 1.2 percent loss assumed as a first guess. It follows that, in order to keep h within the achievable value of $90WK^{-1}m^{-2}$ and allowing a temperature rise of 125K, the copper loss in the primary should not exceed

$$P_{cu} = \frac{90}{102.9} \times 20381 = 17826W$$

If, however, one assumes the 140K temperature rise allowed by IEEE St. 11-1980, then the copper loss in the primary could reach 20000W.

In order to evaluate the electric and magnetic loadings it is necessary to choose a base speed. This is selected on the basis of performance envelope considerations to correspond to a synchronous

speed $n_s$ = 1900 rpm, or f = 63.33 Hz. At this base speed the ideal torque is

$$T_i = \frac{P_i}{2\pi n_s/60} = \frac{1.77\times10^6}{2\pi\times1900/60} = 8895 \text{ N-m}$$

The ideal force density per unit bore surface is

$$KB = \frac{T_i}{\frac{\pi}{2} D^2 L} = \frac{8895}{\frac{\pi}{2} (0.52)^2\times0.45} = 4654 \text{ N/m}^2$$

where K = surface current density = electric loading

B = magnetic flux density = magnetic loading

The physical length of the gap is

$$g' \sim 4.7 \times 10^{-3} \, p^{-1/2} \, D$$

or

$$g' = 4.7 \times 10^{-3} \times \frac{0.52}{\sqrt{2}} = 1.73 \times 10^{-3} \text{m}.$$

This length is not adequate for traction motor applications. A physical length $g' = 2.45 \times 10^{-3}$m is assumed.

To account for the mmf drops in the iron portion of the magnetic path and resulting from the presence of the slots, one introduces an effective air gap length g, such that

$$\frac{g}{D} = 7.25 \times 10^{-3} \, P_i^{0.01} \, p^{-0.5}$$

or

$$\frac{g}{D} = 7.25 \times 10^{-3} \times (1.77 \times 10^6)^{0.01} \, 2^{-0.5} = 5.9 \times 10^{-3}$$

An approximate value for the per unit magnetizing current is given by

$$i_\mu \sim 0.28\ P_i^{-0.1}\ f^{0.15}\ p^{0.6}$$

or

$$i_\mu = 0.28 \times (1.77 \times 10^6)^{-0.1} \times (63.33)^{0.15}\ 2^{0.6} = 0.188$$

The ratio of the magnetic to electric loadings is then according to Ampere's law.

$$\frac{B}{K} = i_\mu \frac{\mu_o}{2p(g/D)}$$

or

$$\frac{B}{K} = 0.188 \frac{4\pi \times 10^{-7}}{2\times2(5.9\times10^{-3})} = 10^{-5}\ \text{H/m}$$

It follows that

$$B = \sqrt{KB(\frac{B}{K})} = \sqrt{45203 \times 10^{-5}} = 0.672\ \text{T}$$

and

$$K = \frac{\sqrt{KB}}{\sqrt{B/D}} = \frac{\sqrt{45203}}{\sqrt{10^{-5}}} = 6.72 \times 10^4\ \text{A/m}.$$

At the assumed operating temperature

$$t = 125 + 40 = 165°C$$

the conductivity is

$$\gamma = \frac{\gamma_{20}}{1+3.81\times10^{-3}(t-20)}$$

where $\gamma_{20}$ = conductivity at 20° centigrade

$t$ = temperature in degrees centigrade

or

$$\gamma = \frac{5.7 \times 10^7}{1+3.81\times10^{-3}\times(165-20)} = 3.67 \times 10^7 \text{ S/m}$$

With the assumed number of slots $Q_1 = 72$, the number of slots per pole and phase is

$$q = \frac{72}{2\times2\times3} = 6$$

and the distribution factor is

$$k_d = \frac{\sin(\pi/6)}{6\sin(\pi/36)} = 0.956$$

With the assumed chording $(W/\tau) = 2/3$ the pitch factor is

$$k_p = \sin\left(\frac{2}{3}\frac{\pi}{2}\right) = 0.866$$

so that the winding factor is

$$k_{dp} = 0.956 \times 0.866 = 0.828$$

It follows that, with the allowable thermal stress and loss, the volume current density is

$$J = \frac{k_{dp}\gamma h\vartheta}{K} = \frac{0.828\times3.67\times10^7\times90\times125}{6.72 \times 10^4} = 5.087 \times 10^6 \text{ A/m}^2$$

and the effective conductor thickness is

$$a = \frac{K}{Jk_{dp}} \quad \frac{6.72\times10^4}{5.087\times10^6\times0.828} = 1.595 \times 10^{-2} \text{ m}$$

The relative thickness of the conductor is then,

$$\frac{a}{D} = \frac{1.595\times10^{-2}}{0.52} = 3.06 \times 10^{-2}$$

At this point it is important to check the heights of the slots and stator core. Assuming a slot filling coefficient $k_{cu} = 0.5$ one obtains a slot height

$$h_s = \frac{a}{k_{cu}} \frac{\tau_s}{w_s} = \frac{1.595\times10^{-2}}{0.5\times0.5} = 6.38 \times 10^{-2} m$$

This value gives an average slot pitch

$$\tau_{save} = \frac{D+h_s}{D} \tau_s = \frac{0.52+0.0638}{0.52} \tau_s = 1.12 \tau_s$$

which is consistent with the previously assumed value $\tau_{save} = 1.1 \tau_s$.

The height available for the core is then

$$h_c = \frac{D_o-2h_s-D}{2} = \frac{0.83-2\times0.0638-0.52}{2} = 0.0912 \text{ m}$$

One must now verify if this height is adequate to carry the core flux

$$\Phi_c = \frac{\Phi_g}{2} + \Phi_\ell = (1 + \sigma_1) \frac{\Phi_g}{2}$$

where $\Phi_g$ = magnetic flux at the gap

$\sigma_1$ = $X_1/X_m$ = leakage coefficient

$X_1$ = leakage reactance of the primary

$X_m$ = magnetizing reactance.

The leakage coefficient is given approximately by

$$\sigma_1 = 0.02 + 0.0038\ p$$

or

$$\sigma_1 = 0.02 + 0.0038 \times 2 = 0.0276$$

Assuming a ratio $(L/\ell_{Fe}) = 1.03$ in the effective to iron length of the lamination stack and a ratio $f_B = 1.1$ in the rms to average values of B, the magnetic flux density in the core is

$$B_c = \frac{\Phi_c}{h_c}\frac{1}{\ell_{Fe}} = (1+\sigma_1)\ (\frac{\pi D}{2p})\ (\frac{L}{\Pi_{Fe}})\ \frac{1}{2h_c}\ \frac{B}{f_B}$$

$$B_c = (1+0.0276)\ (\frac{\pi \times 0.52}{2 \times 2}) \times 1.03 \times \frac{1}{2 \times 0.0912} \times \frac{0.672}{1.1} = 1.44\ T$$

This flux density exceeds the recommended value of 1.2 T by 20 percent. It could be reduced by decreasing $h_s$. This, however, would require a larger $w_s$ resulting in a higher flux density in the teeth and longer end windings. These could not be accommodated in the available space. A better option, in view of the low value of assumed copper loss and temperature rise, would be to reduce $h_s$ by selecting a higher J.

This completes the basic design.

Appendix V

# APPENDIX V

## 1. Determination of the Motor Torque and Power

It is assumed that the electric vehicle has the following parameters:

| | |
|---|---|
| gross vehicle mass | $m = 1770$ kg |
| drag coefficient | $C_d = 0.3$ |
| frontal area | $A = 1.8\ m^2$ |
| tire pressure | $p = 221$ kPa |
| wheel radius | $r_w = 0.28$ m |

and must attain the following performance objectives:

Urban Traffic: SAE J227a Schedule D Cycle (Fig.1)

Highway Traffic:

| | |
|---|---|
| passing speed | 70 mph (31.28 m/s) |
| cruising speed | 55 mph (24.64 m/s) |
| 0-30 mph acceleration | 9s |
| 25-55 mph acceleration (thruway merging duty) | 18s |
| Speed on 5% grade | 50 mph (22.4 m/s) |
| Speed on 10% grade | 15 mph (7 m/s) |

The toughest performance requirement is thruway access. For this the acceleration

$$a = 1.9 \exp [ - 0.065t ]$$

is chosen. This leads to the desired speed of 24.64 m/s (55mph) in 28 s. It also satisfies the separate requirements of acceleration from 0 to 30 mph in 9s and the thruway merging duty acceleration from 25 to 55 mph in 18 s. An exponentially decaying acceleration was chosen, rather than a constant one, in order to reduce the peak power drawn from the battery at the expense of a somewhat more stringent requirement on the torque developed by the motor at starting.

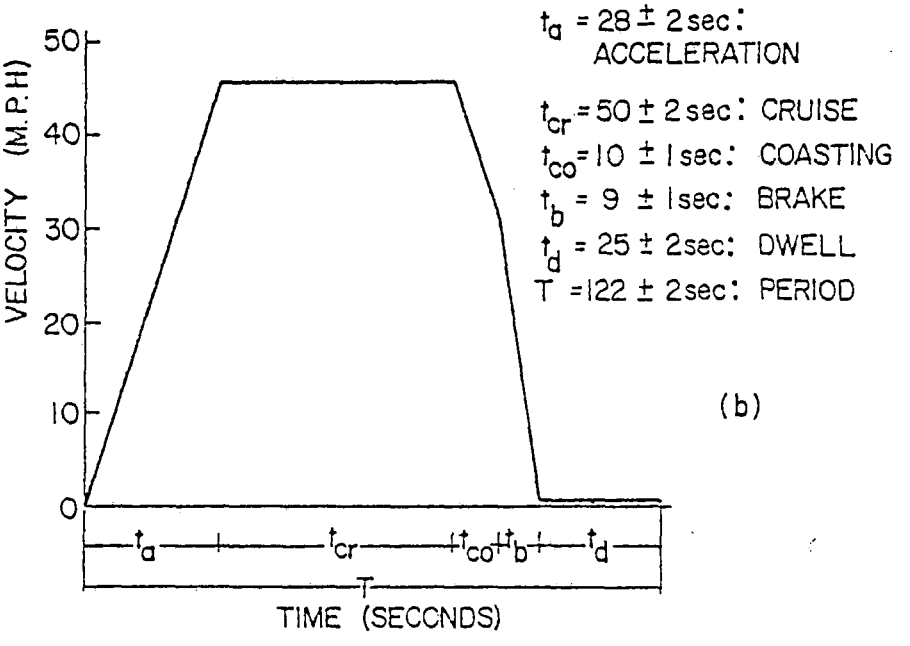


Fig. 1 SAE J227a Schedule D Cycle for passenger electric vehicle

The acceleration

$$a = 1.22 \exp [ - 0.042 t ]$$

was chosen for the SAE cycle. It leads to the desired 20.2 m/s speed in 28 s.

According to the SAE cycle, the car has to be brought to a halt from 20.2 m/s in 19 s. Part of the kinetic energy can be fed back by operating the propulsion system in the generating mode. Again, in order to avoid a large peak of power, the deceleration rate is chosen to vary exponentially as:

$$a = - 0.5 \exp [ 0.071t ]$$

One can now take advantage of the fact that an exponentially decaying acceleration

$$a = a_o e^{-t/\tau}$$

gives the linear relation

$$a = a_o - \frac{v}{\tau}$$

between acceleration and speed, and express the acceleration rates corresponding to the various performance specifications in terms of the speed. The overall tractive effort T.E. is then obtained as a function of the speed, by summing up the components of the resistance to motion.

The inertia component is

$$R_a = m*a$$

where m* is an equivalent mass which accounts for the inertia of the rotating masses as follows.

$$m^* = \begin{cases} 1.1\ m \text{ for passenger vehicles in low gear} \\ 1.05\ m \text{ for passenger vehicles in high gear} \end{cases}$$

and m is the vehicle mass.

The gradability component is

$$R_g = m\ g\ \sin\vartheta$$

where $g = 9.81\ m/s^2$ = acceleration of gravity

$\vartheta$ = grade angle

The aerodynamic drag is

$$R_d = \left(\frac{1}{2}\ \xi v^2\right) C_d\ A$$

where $\xi = 1.243\ kg/m^3$

$C_d$ = drag coefficient

A = frontal area.

The rolling resistance for steel belted radial tires is

$$R_r = \left(5 \times 10^{-3} + \frac{10^3}{p} + \frac{0.36v^2}{p}\right) mg$$

where p = tire pressure $\sim 2.2 \times 10^5$ Pa

The tractive effort T.E. can be transformed into an expression relating the torque at the wheel $T_w$ to the revolutions per minute $n_w$ by introducing the wheel radius $r_w$, so that

$$T_w = r_w \times T.E.$$

and

$$v = 2\pi r_w \frac{n_w}{60}$$

The losses in the gear, differential, and axle can be estimated at 4 percent of the useful torque. This should be taken into account in specifying the motor output. The torque and power requirements augmented by the 4 percent loss are shown in Fig. 2.

The data points marked A correspond to the thruway acceleration requirements, points marked S denote the SAE cycle acceleration and points marked C indicate the cruising requirements. The gradability requirements lead to the points G which, as can be seen, fall well within the acceleration torque and power envelopes.

In contrast the power required for thruway passing cannot be provided economically, even if it is calculated on the basis of specifications which are inadequate to ensure safety. This can be deduced from the value of the torque represented by point P in Fig. 2.

It is interesting to note that the torque points A, S, and C lie approximately on straight lines and, therefore, lead to convenient analytical expressions as follows:

$$T_{wA} = 1139 - 1.035n$$

$$T_{wS} = 749 - 0.663\ n_w$$

$$T_{wC} = 0.14\ n_w$$

The corresponding powers are:

$$P_A = \frac{2\pi}{60}\ n_w\ T_{wA} = 119.25\ n_w - 0.108\ n_w^2$$

$$P_S = \frac{2\pi}{60}\ n_w\ T_{wS} = 78.42\ n_w - 0.069\ n_w^2$$

$$P_C = \frac{2\pi}{60}\ n_w\ T_{wS} = 0.0146\ n_w^2$$

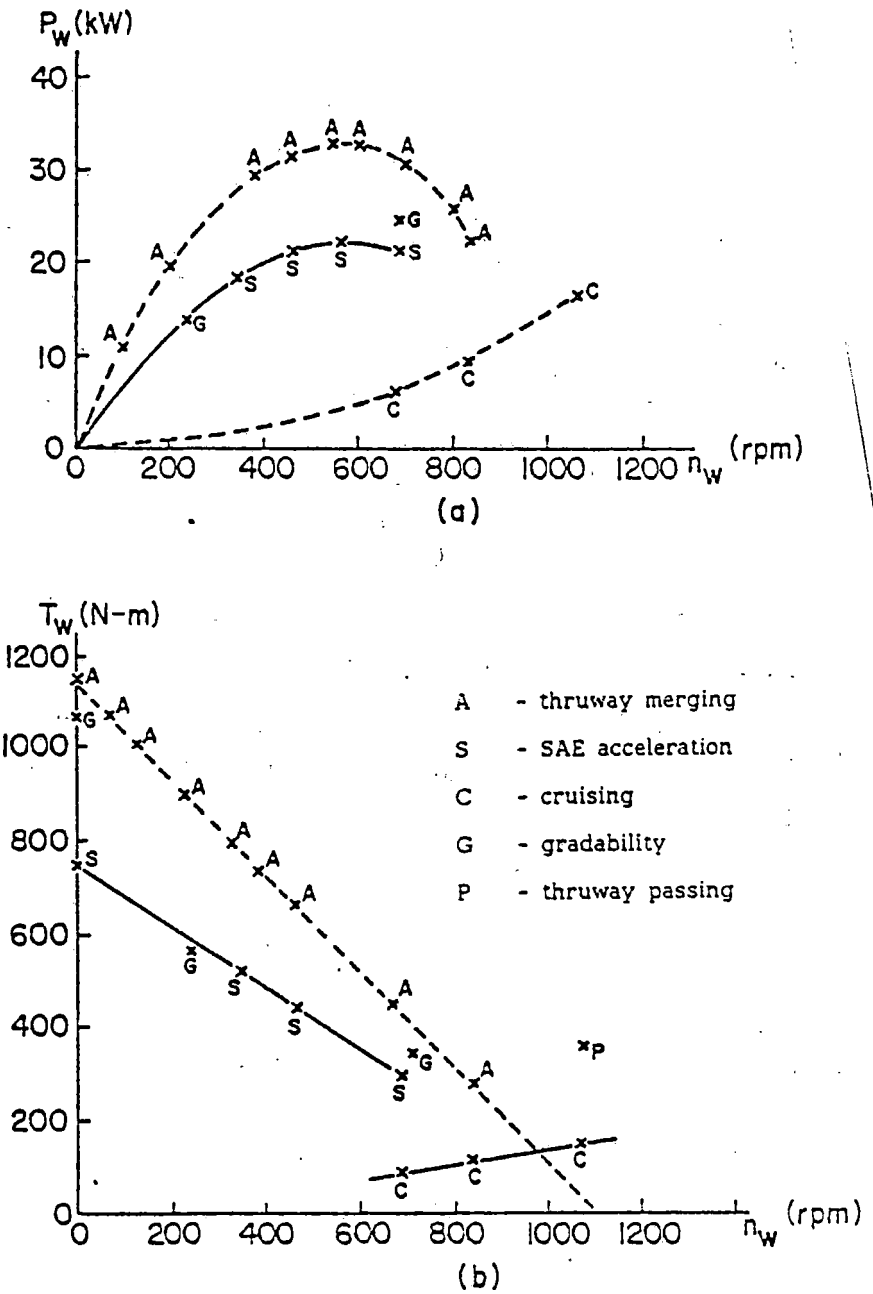


Fig. 2 Augmented performance requirements at wheel as a function of its speed: (a) torque, (b) power

Similarly one obtains for the braking requirements:

$$T_{wB} = - 974.33 + 1.16\ n_w$$

$$P_{wB} = -102\ n_w + 0.1214\ n_w^2$$

It appears that the maximum torque occurs at stalling and is $T_{wmax} = 1139$ N-m.

The maximum power is $P_{wmax} = 32.92$ kW.

2. Determination of the Bore Surface

It is desired to use a squirrel-cage induction motor and a two-speed gear box. Considerations, primarily based on the noise level, limit the motor speed at 9000 rpm. The passing speed of 112 km/h (70 mph) dictates a maximum wheel speed $n_w = 1067$ rpm. The high-gear ratio is then

$$r_H = \frac{n_{max}}{n_{wmax}} = \frac{9000}{1067} = 8.435$$

The major consideration in choosing the low-gear ratio is that the gear shift should be smooth. This imposes the condition that the wheel torque-speed curve in low-gear intersect the torque-speed curve in high-gear before the motor reaches $n_{max}$. According to Fig. 3, this corresponds to the condition

$$\frac{n_{max}}{r_L} > \frac{n_b}{r_H}$$

or

$$\frac{r_L}{r_H} < \frac{n_{max}}{n_b}$$

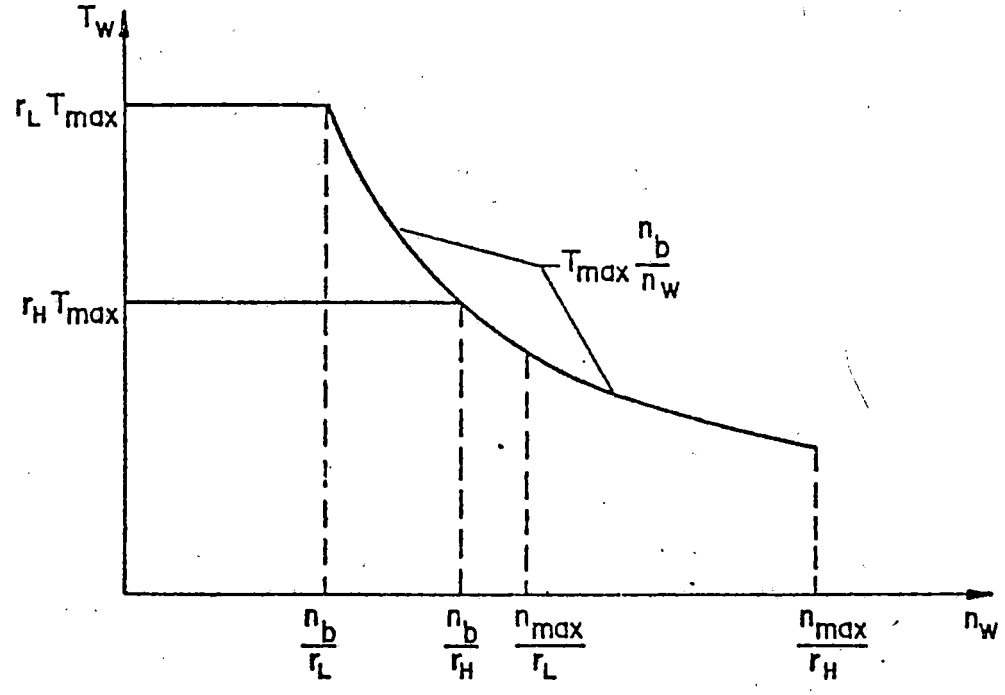


Fig. 3 Torque-speed characteristic at the wheel in low and high gears.

so that $$r_L < \frac{8.435 \times 9000}{n_b} = \frac{75915}{n_b}$$

A second relation is obtained by observing that the constant power portion of the curve must correspond to the maximum power demand and that $T_{max}$ must equal $T_{st}/r_L$. It follows that

$$T_w = \frac{P_{max}}{2\pi n_w/60} = T_{max} \frac{n_b}{n_w} = \frac{T_{st}}{r_L} \frac{n_b}{n_w}$$

or

$$r_L = \frac{2\pi T_{st}}{60 P_{max}} n_b = 0.1047 \frac{T_{st}}{P_{max}} n_b$$

Assuming $T_{st}$ = 1200 N-m, and $P_{max}$ = 35 kW, in order to allow some margin in the performance, yields

$$r_L = 0.1047 \frac{1200}{35000} n_b = 0.00359 \, n_b < \frac{75915}{n_b}$$

or $$n_b < \sqrt{\frac{75915}{0.00359}} = 4598.5$$

The base speed is chosen to be 4555 rpm. This yields

$$r_L = 0.00359 \times 4555 = 16.35$$

The motor is supplied through a transistorized PWM inverter with a 180° conduction period from a 144 V battery. It is estimated that the voltage drop caused by the internal resistance of the battery, the connecting cables, and the primary resistance of the motor is 0.12 per unit or 17.28 V. The forward voltage drop of the transistors is 4 V.

In the case of a voltage source inverter with a 180° conduction period the following relations hold between phase and dc voltages

$$V_{ph} = \frac{\sqrt{2}}{\pi} V_{dc}$$

Since the battery does not "see" the motor reactances, the effective emf is

$$e = \frac{R'_2}{S} I'_2 \sim \frac{\sqrt{2}}{\pi} (144 - 17.28 - 4) = 55.1 \text{ V}$$

where $R'_2$ = secondary resistance referred to the primary

$I'_2$ = secondary current referred to the primary

$S$ = slip

Making use of Faraday's law

$$e = 2\pi f N_{eff} \Phi = \frac{2\pi}{60} nr N_{eff} p \Phi$$

where $N_{eff}$ = effective number of turns

$\Phi$ = flux per pole = $\frac{DL}{p} B$

$p$ = number of pole pairs

$D$ = bore diameter

$L$ = effective bore length

$B$ = magnetic flux density of the gap

one obtains the total flux interlinkage

$$p N_{eff} \Phi = \frac{55.1 \times 60}{2\pi \chi 4555} = 0.1155 \text{ Wb}$$

This corresponds to a secondary current

$$I_2' = \frac{T}{m_1 p N_{eff} \Phi} = \frac{1200}{16.35 \times 3 \times 0.1155} = 212A$$

where $m_1$ = number of primary phases.

By conservation of energy one obtains for the dc current

$$I_{dc} = \frac{\sqrt{2} \times 3}{\pi} \; 212 = 286.3A.$$

At base speed the iron is highly saturated and one may assume $B = 0.56T$, so that

$$N_{eff} DL = \frac{0.1155}{0.56} = 0.206 \; m^2$$

It is interesting to note that this result has been obtained without the need to specify the number of poles. This is chosen equal to two, in order to have low frequency and, therefore, low iron core losses in the motor and low switching stresses and losses in the inverter. The frequency at maximum speed is then 150Hz. The partition between $N_{eff}$ and the bore dimensions is decided by thermal considerations which will be discussed later on. One can, however, carry the calculations one step further.

First one should note that although the calculations were made on the basis of the emf across the resistance $R_2'/S$, the effective number of turns is that of the primary, because all secondary quantities are referred to the primary. It is assumed that the number of primary slots is $Q_1 = 36$ and that the coil throw is $W/\tau = 7/9$. The distribution and pitch factors are then

$$k_d = 0.956 \qquad \text{and} \qquad k_p = 0.94$$

so that

$$NDL = \frac{0.206}{0.956 \times 0.94} = 0.229$$

If the winding is arranged in two layers there are 12 coils per phase, i.e. N = 12 for one turn per coil, N = 24 for two turns per coil and so on. The choices are, therefore, limited to

$$DL = \frac{0.229}{12N_c} = \frac{0.019}{N_c}$$

In this particular machine it will turn out that it is practical to choose either $N_c = 1$ or $N_c = 2$, resulting in two designs in which the bore surface differs by a factor of 2.

3. Determination of the Main Parameters

The temperature rise of the winding is calculated on the basis of the SAE duty cycle which has an on-time/period ratio of 97/122 seconds with a power requirement

$$P_S = 78.42\ n_w - 0.069\ n_w^2$$

It is assumed that the primary current and, therefore the copper losses are maintained practically constant at the value corresponding to the peak power which occurs at $n_w = 568.26$ with a value $P_{Smax} = 22281$ W. Assuming $\eta = 0.85$ and cos $\phi$ 0.88 one obtains an ideal power

$$P_i = \frac{P_R}{\eta \cos\phi} = \frac{22281}{0.85 \times 0.88} = 29787 \text{ W}$$

The primary copper loss is then estimated as

$$P_{cu1} = 0.42\ P_R^{0.75} = 0.42\ (29787)^{0.75} = 952\ W.$$

This corresponds to an average loss over the SAE duty cycle

$$P_{cu} = P_{cu1}\ \frac{\text{on-time}}{\text{period}} = 952\ \frac{97}{122} = 757\ W$$

In a passenger electric vehicle weight should be kept at a minimum. For this purpose, a large aspect ratio, say L/D = 1.9, is chosen. The relative conductor length is then

$$\frac{\ell_{co}}{L} \sim 1 + \frac{2D}{pL} = 1 + \frac{2}{1.9} = 2.05$$

The power dissipated per unit surface is

$$p_{s\text{-}diss} = \frac{P_{cu}(L/\ell_{co})}{\pi DL} = \frac{757}{2.05\times\pi\times0.019}\ N_c = 6186\ N_c\ [W/m^2]$$

In steady state

$$p_{s\text{-}diss} = h\vartheta_w$$

where h = overall heat transfer coefficient

$\vartheta_w$ = temperature rise of the winding.

Selecting a totally enclosed construction and assuming an operating temperature rise equal to 2/3 of the maximum allowable $\vartheta_w$, one obtains for class H insulation,

$$\vartheta_w = \frac{2}{3} \times 125 = 83.3\ K$$

The corresponding overall heat transfer coefficient is then

$$h = \frac{6186\ N_c}{83.3} = 74.2\ N_c\ [WK^{-1}m^{-2}]$$

Even selecting $N_c = 1$, such a heat transfer coefficient cannot be achieved with air ventilation, but it can be attained with external oil cooling.

The bore dimensions are then:

$$D = 0.1\ m$$

$$L = 0.19\ m$$

Considering the strong accelerations (g's) to which a traction motor is subjected, a large air gap length must be chosen. A physical gap length $g' = 1.2\times 10^{-3}$m is selected. This large air gap gives rise to a relatively large per unit magnetizing current, which turns out to be

$$I_\mu = 0.377$$

Making use of Ampere's law, one can then obtain the ratio between magnetic and electric loadings

$$\frac{B}{K} = i_\mu \frac{\mu_o}{2p(g/D)}$$

or

$$\frac{B}{K} = 0.377 \frac{4\pi\times 10^{-7}}{2\times 0.0142} = 1.67 \times 10^{-5}\ H/m$$

The motor torque at peak power is:

$$T = \frac{P_R}{\Omega} = \frac{22281}{2\pi\times 568.26\times 8.435/60} = 44.38\ N\text{-}m$$

Equating this expression for the torque with

$$T = \frac{P}{w/p} = \frac{\pi}{2} D^2 LKB \cos\alpha \sim \frac{\pi}{2} D^2 LKB \cos\phi$$

one obtains

$$KB = \frac{44.38}{\frac{\pi}{2}(0.1)^2 \times 0.19 \times 0.88} = 16897 \text{ N/m}^2$$

so that

$$B = \sqrt{KB\left(\frac{B}{K}\right)} = \sqrt{16897 \times 1.67 \times 10^{-5}} = 0.531 \text{ T}$$

and

$$K = \sqrt{\frac{KB}{B/K}} = \frac{\sqrt{16897}}{\sqrt{1.67 \times 10^{-5}}} = 31810 \text{ A/m}$$

At the assumed operating temperature

$$t = 83.3 + 40 = 123.3°C$$

the conductivity is

$$\gamma = \frac{5.7 \times 10^{-7}}{1 + 3.81 \times 10^{-3} \times (123.3 - 20)} = 4.09 \times 10^7 \text{ S/m}$$

so that one obtains

$$J = \frac{k_{dp} \gamma h \delta_w}{K} = \frac{0.899 \times 4.09 \times 10^7 \times 6186}{31810} = 7.15 \times 10^7 \text{ A/m}^2$$

The equivalent thickness of the conductor is then

$$a = \frac{K}{J k_{dp}} \quad \frac{31810}{7.15 \times 10^7 \times 0.899} = 4.948 \times 10^{-3} \text{ m.}$$

and

$$\frac{a}{D} = \frac{4.948\times10^{-3}}{0.1} = 4.948 \times 10^{-2}$$

The phase current can be found as

$$I_{ph} = \frac{\pi DK}{2mN_{eff}} \quad \frac{31810\times\pi\times0.1}{2\times3\times12\times0.899} = 154.39 \text{ A.}$$

This completes the basic design.

**Optimization of the Design of Electric Traction Motors for Railroad and Other Applications**, 1983
E. Levi